



The University of  
**Nottingham**

UNITED KINGDOM · CHINA · MALAYSIA

Jennings, James and He, Guping and Howdle, Steven M. and Zetterlund, Per B. (2016) Block copolymer synthesis by controlled/living radical polymerisation in heterogeneous systems. *Chemical Society Reviews* . ISSN 1460-4744

**Access from the University of Nottingham repository:**

[http://eprints.nottingham.ac.uk/35122/1/JJenningsCSR\\_BCP\\_071416.pdf](http://eprints.nottingham.ac.uk/35122/1/JJenningsCSR_BCP_071416.pdf)

**Copyright and reuse:**

The Nottingham ePrints service makes this work by researchers of the University of Nottingham available open access under the following conditions.

This article is made available under the University of Nottingham End User licence and may be reused according to the conditions of the licence. For more details see: [http://eprints.nottingham.ac.uk/end\\_user\\_agreement.pdf](http://eprints.nottingham.ac.uk/end_user_agreement.pdf)

**A note on versions:**

The version presented here may differ from the published version or from the version of record. If you wish to cite this item you are advised to consult the publisher's version. Please see the repository url above for details on accessing the published version and note that access may require a subscription.

For more information, please contact [eprints@nottingham.ac.uk](mailto:eprints@nottingham.ac.uk)

# Block Copolymer Synthesis by Controlled/Living Radical Polymerisation in Heterogeneous Systems

J. Jennings,<sup>1,2,\*</sup> G. He,<sup>1</sup> S. M. Howdle,<sup>1</sup> P. B. Zetterlund<sup>3</sup>

<sup>1</sup>*School of Chemistry, University of Nottingham, University Park, Nottingham, UK*

<sup>2</sup>*Department of Chemistry, University of Wisconsin—Madison, Madison, Wisconsin, 53706, United States*

<sup>3</sup>*Centre for Advanced Macromolecular Design (CAMD), School of Chemical Engineering, The University of New South Wales, Sydney, NSW 2052, Australia*

## Abstract

Nanostructured soft materials open up new opportunities in material design and application, and block copolymer self-assembly is one particularly powerful phenomenon that can be exploited for their synthesis. The advent of controlled/living radical polymerisation (CLRP) has greatly simplified block copolymer synthesis, and versatility towards monomer types and polymer architectures across the different forms of CLRP has vastly expanded the range of functional materials accessible. CLRP-controlled synthesis of block copolymers has been applied in heterogeneous systems, motivated by the numerous process advantages and the position of emulsion polymerisation at the forefront of industrial latex synthesis. In addition to the inherent environmental advantages of heterogeneous routes, the incidence of block copolymer self-assembly within dispersed particles during polymerisation leads to novel nanostructured materials that offer enticing prospects for entirely new applications of block copolymers. Here, we review the range of block copolymers prepared by heterogeneous CLRP techniques, evaluate the methods applied to maximise purity of the products, and summarise the unique nanoscale morphologies resulting from *in situ* self-assembly, before discussing future opportunities within the field.

## List of abbreviations

4AM	4-Acrylomorpholine
4VP	4-Vinyl pyridine
AA	Acrylic acid
AAEMA	Acetoacetoxyethyl methacrylate
AAM	Acrylamide
AGET	Activator generated by electron transfer
AIBN	$\alpha$ -Azobisisobutyronitrile
ATRP	Atom transfer radical polymerisation
Bd	Butadiene
BCP	Block copolymer
<sup>n</sup> BuMA	n-Butyl methacrylate
<sup>t</sup> BuA	tert-Butyl acrylate
<sup>t</sup> BuMA	tert-Butyl methacrylate
BzMA	Benzyl methacrylate
CLRP	Controlled/living radical polymerisation
<b>CMRP</b>	<b>Cobalt-mediated radical polymerisation</b>
CTA	Chain transfer agent
CTAB	Cetyltrimethylammonium bromide
C <sub>tr</sub>	Chain transfer constant
Đ	Dispersity
DEAA	N,N'-diethylacrylamide
DEGMA	Di(ethylene glycol) methyl ether methacrylate
DMA	N,N-dimethyl acrylamide
DEAEMA	N,N-diethylaminoethyl methacrylate
DMAEMA	N,N-dimethylaminoethyl methacrylate
DP	Degree of polymerisation
DTB	Dithiobenzoate
DVB	Divinylbenzene
EEMA	2-ethoxyethyl methacrylate
EGDMA	Ethylene glycol dimethacrylate
EISA	Evaporation-induced self-assembly
FMA	2,2,2-trifluoroethyl methacrylate
GIMA	Glycidyl methacrylate
GMA	Glycerol monomethacrylate
GPC	Gel permeation chromatography
GPEC	Gradient polymer elution chromatography
<sup>n</sup> HA	n-hexyl acrylate
HEAA	N-hydroxyethyl acrylamide
HEMA	Hydroxyethyl methacrylate
HPLC	High performance liquid chromatography
HPMA	2-hydroxypropyl methacrylate
<sup>i</sup> BuMA	iso-Butyl methacrylate
LAC	Liquid adsorption chromatography
LCST	Lower critical solution temperature
MA	Methyl acrylate
MAA	Methacrylic acid
MAAm	Methacrylamide

MBA	N,N'-methylenebisacrylamide
MEA	2-methoxyethyl acrylate
MMA	Methyl methacrylate
MW	Molecular weight
MWD	Molecular weight distribution
NaMA	Sodium methacrylate
NIPAM	N-isopropyl acrylamide
NMP	Nitroxide mediated radical polymerisation
NMR	Nuclear magnetic resonance
OEGMA	Oligo(ethylene glycol) methyl ether methacrylate
PDMS-MA	Poly(dimethylsiloxane) monomethacrylate
PEG	Polyethylene glycol
PEGA	poly(ethylene glycol) methyl ether acrylate
PEGMA	poly(ethylene glycol) methyl ether methacrylate
PISA	Polymerisation-induced self-assembly
PMPC	Poly(2-(methacryloyloxy)ethyl phosphorylcholine)
PNaA	Polysodium acrylate
QD	Quantum dot
RAFT	Reversible addition-fragmentation chain transfer
RI	Refractive index
RITP	Reverse iodine transfer polymerisation
RTCP	Reversible chain transfer catalysed polymerisation
SAN	Styrene-co-acrylonitrile
SARA-ATRP	Supplemental activator and reducing agent atom transfer radical polymerisation
SBAS	Styrene-butyl acrylate-styrene triblock copolymer
SBS	Styrene-butadiene-styrene triblock copolymer
scCO <sub>2</sub>	Supercritical carbon dioxide
SDS	Sodium dodecyl sulfate
SET-LRP	Single-electron transfer living radical polymerisation
SMA	Styrene-alt-maleic anhydride copolymer
SORP	Self-organised reprecipitation
SS	Styrene sulfonate
St	Styrene
TEDETA	Tetraethyldiethylenetriamine
TEM	Transmission electron microscopy
TERP	Organotellurium-mediated living radical polymerisation
THF	Tetrahydrofuran
T <sub>g</sub>	Glass Transition Temperature
TLC	Thin Layer Chromatography
TPE	Thermoplastic elastomer
TTAB	n-tetradecyltrimethylammonium bromide
TTC	Trithiocarbonate
VDC	Vinylidene chloride
VOC	Volatile organic compound
$\chi$	Flory-Huggins polymer-polymer interaction parameter

## 1. Introduction

### 1.a. Heterogeneous polymerisation classes

The simplest way, conceptually, to conduct a radical polymerisation is as a homogeneous system in bulk or solution. However, for reasons that will be explained in Section 1b, it is very advantageous to conduct radical polymerisation in heterogeneous systems. These systems typically constitute a dispersed phase surrounded by a continuous medium which is most commonly, but not always, water. The various types of heterogeneous polymerisation systems are: emulsion,<sup>1,2</sup> miniemulsion,<sup>3-5</sup> microemulsion,<sup>6,7</sup> precipitation,<sup>8</sup> dispersion<sup>9-11</sup> and suspension<sup>12</sup> polymerisations. Systems where the continuous phase is organic (hydrophobic) and the dispersed phase is hydrophilic are referred to as inverse systems, *e.g.* inverse miniemulsion polymerisation.<sup>13</sup> In dispersion polymerisations, the continuous phase is typically comprised of water/alcohol mixtures, and supercritical CO<sub>2</sub> (scCO<sub>2</sub>) can also be used in both precipitation and dispersion polymerisations.<sup>14-16</sup> In what follows, brief descriptions of the different types of heterogeneous systems will be provided. It should be pointed out that the features outlined below typically apply to conventional radical polymerisation, and some of these characteristics may be different in case of controlled/living radical polymerisation (CLRP), which is discussed in Section 1d. This is illustrated by, for example, considering how non-living dispersion polymerisations normally yield close to monodisperse particles, whereas dispersion CLRP typically gives broad particle size distributions (unless specific approaches are employed).<sup>17</sup> Although IUPAC recommends the term “reversible deactivation radical polymerisation” (RDRP),<sup>18</sup> the older term CLRP is employed in this review to minimise confusion.

An *emulsion polymerisation* (often referred to as *ab initio* emulsion) is attractive in its simplicity of preparation – one simply stirs a mixture of water, initiator (most frequently water-soluble), monomer and surfactant at elevated temperature. From a mechanistic perspective, the polymerisation is divided into three well-defined intervals depending on monomer conversion: Interval I (approx. 0-10% conv.): Polymer particles are formed in the aqueous phase via micellar or homogeneous nucleation; Interval II (approx. 10-40% conv.): Monomer droplets and monomer-swollen particles coexist, and diffusion from droplets to particles occurs as monomer reacts in the particles by polymerisation; Interval III (approx. conv. > 40%): The monomer droplets have now been consumed, and the system comprises monomer-swollen particles in an aqueous continuous phase. Emulsion polymerisation typically results in particle

diameters  $d \approx 80\text{-}600$  nm with relatively narrow particle size distributions. A *miniemulsion polymerisation* is mechanistically very different from an emulsion polymerisation – in the former, polymer particles are formed via monomer droplet nucleation (polymerisation in monomer droplets). Ideally, each monomer droplet is converted to its corresponding polymer particle. To make monomer droplet nucleation possible, it is a requirement that the droplet size is sufficiently small to ensure the droplets can capture all aqueous radicals (in case of water-soluble initiators). **The surfactant concentration should be high enough to provide adequate monomer droplet stabilization, but sufficiently low such that surfactant micelles are not present.** A typical recipe consists of water, surfactant, monomer, water- or oil-soluble initiator, and usually a hydrophobe (*e.g.* hexadecane) to minimise Ostwald ripening.<sup>19</sup> The initial mixture is subjected to external shear forces via ultrasonication or microfluidisation, resulting in thermodynamically unstable but kinetically stable monomer droplets. Miniemulsion polymerisation typically generates relatively broad particle size distributions with  $d \approx 60\text{-}300$  nm. In a *microemulsion polymerisation*, polymerisation occurs inside monomer-swollen micelles. A microemulsion is a thermodynamically stable and transparent or translucent emulsion that forms spontaneously on mixing of an aqueous surfactant solution with monomer and sometimes a cosurfactant (*e.g.* 1-pentanol). The surfactant content in a microemulsion polymerisation is much higher than in all other systems described in this section, and typically results in particles with  $d \approx 10\text{-}60$  nm. In a *precipitation polymerisation*, all components are initially soluble in the continuous phase, which normally comprises an alcohol/water mixture. As polymer chains grow, a critical chain-length is eventually reached at which solubility diminishes and precipitation occurs, resulting in particle formation with  $d \approx 100\text{-}600$  nm. A *dispersion polymerisation* is essentially the same as a precipitation polymerisation, but with the addition of a stabiliser. Normally, steric stabilisers such as poly(vinylpyrrolidone) or diblock copolymers are employed. Precipitation occurs as the critical chain-length is reached, leading to formation of unstable precursor particles, which then coalesce and adsorb stabilisers yielding stable polymer particles. Dispersion polymerisations often result in narrower particle size distributions than precipitation polymerisations and  $d \geq 1\mu\text{m}$ . A *suspension polymerisation* is conceptually similar to a miniemulsion polymerisation in that polymerisation occurs in pre-formed monomer droplets. However, the stirring applied is not high energy (*i.e.* not ultrasonication) and as such the monomer droplets are very large. Initiation occurs via oil-soluble initiators inside the monomer droplets, yielding very large polymer particles with  $d$  ranging from  $\mu\text{m}$  to mm.

## 1.b. Why heterogeneous polymerisation?

Dispersed systems, in particular emulsion polymerisations, are preferred for industrial polymer synthesis due to ease of large scale implementation; advantages include low environmental impact (usually an aqueous continuous phase), good heat transfer and low viscosity. Direct use of the final latex is often possible, and the ability to create polymeric particles of various morphologies is desirable for a wide range of potential applications. Furthermore, in an emulsion polymerisation, the system can be taken to very high monomer conversion without any concomitant increase in the overall viscosity. On the contrary, polymerisation in bulk or in high monomer concentration solutions leads to solidification of the polymerisation mixture, and additional processing steps are required to recover the polymer. Moreover, emulsion polymerisation often affords high molecular weight polymers in short reaction times due to effects of compartmentalisation, whilst in homogeneous systems such as bulk and solution, an increased initiator concentration is required to achieve high polymerisation rate, which inevitably leads to lower molecular weight polymer.<sup>1, 2</sup> This is a considerable drawback, because obtaining polymers of high molecular weight is usually advantageous from a materials properties viewpoint. A vast number of polymeric products are produced industrially *via* emulsion polymerisation, e.g. various rubbers such as styrene-butadiene rubber, certain grades of polystyrene and poly(methyl methacrylate), as well as poly(vinyl chloride) and poly(vinylidene chloride). The ability to produce polymeric nano/microparticles using the “bottom-up” approach of a one-pot heterogeneous polymerisation is arguably the key to their widespread industrial success. Furthermore, the importance of polymeric particles for various high-tech applications cannot be overstated – such applications embody diverse areas in material science, health care products and nanomedicine.

### 1.c. Block copolymer synthesis by CLRP

In a conventional “non-living” radical polymerisation, the time that passes between initiation of a given chain and its chain-end forming event (bimolecular termination or chain transfer) is typically of the order of 1 second. Different chains are initiated and undergo chain-end forming events throughout the polymerisation process – under such conditions it is impossible to precisely control macromolecular architecture and create distinct sequences of monomers (*i.e.* block copolymers). However in CLRP, the lifetime of a growing chain is extended to last throughout the polymerisation process (typically the order of hours). Importantly, the dormant or “living” chain ends can be re-activated, thus enabling chain extension with a different monomer to create well-defined block copolymers. The fundamental principles of CLRP are most elegantly explained in the introduction of the excellent review by Goto and Fukuda in 2004.<sup>20</sup> The three most common CLRP methods are nitroxide-mediated radical polymerisation (NMP),<sup>21</sup> atom transfer radical polymerisation (ATRP)<sup>22</sup> and reversible addition-fragmentation chain transfer (RAFT) polymerisation.<sup>23</sup> NMP and ATRP operate via the so called persistent radical effect, whereas RAFT (and the closely related organotellurium-mediated living radical polymerisation, TERP) is based on degenerative transfer to obtain control/livingness.

Prior to the advent of CLRP, block copolymers **based on vinyl monomers** could only be prepared *via* living anionic polymerisation.<sup>24</sup> Although anionic systems offer high levels of control over chain architecture, the process is demanding experimentally in that it requires stringent conditions, is highly intolerant to impurities and various functionalities that may be present in the monomer, and offers very limited flexibility. CLRP is thus extremely attractive since it features the robust nature, tolerance and flexibility of radical polymerisation combined with precision and control similar to living anionic polymerisation. In recent years, increasing efforts have been directed towards exact control of the monomer sequence distribution in synthetic polymers.<sup>25</sup> As a step towards this elusive goal, iterative CLRP approaches have been developed for synthesis of high-order multiblock copolymers, whereby each polymerisation step (*i.e.* each block) is taken to near full conversion, followed by simple addition of monomer for the next block in one pot. These approaches are based on maintaining a very high degree of livingness (*i.e.* high blocking efficiency) throughout the polymerisation either by using Cu(0)-mediated radical polymerisation<sup>26-28</sup> (known as SARA-ATRP<sup>29</sup> or SET-LRP<sup>30</sup>) or by employing RAFT polymerisation under carefully optimised conditions such that the number of dead chains is very small relative to the number of RAFT end groups.<sup>31-36</sup>



#### 1.d. CLRP in dispersed systems

CLRP was first developed in homogeneous systems (bulk, solution)<sup>21, 23, 37, 38</sup> and demonstrated for the synthesis of various structurally advanced and well-defined macromolecules such as block copolymers, star (co)polymers and other more complex architectures.<sup>26, 31, 36, 39</sup> However, it was soon realised that in order for its full potential to be reached, it was crucial to make CLRP compatible with heterogeneous (dispersed) systems. There are numerous reviews on CLRP in dispersed systems,<sup>3, 40-49</sup> and notably Zetterlund et al.<sup>50, 51</sup> published a comprehensive updated review in 2015. Cunningham and Monteiro published a review in 2012 with a focus on the prospects of commercial development of CLRP in dispersed systems.<sup>52</sup>

It is now possible to conduct CLRP in a very wide range of dispersed systems, including *ab initio* (and seeded) emulsion, miniemulsion, microemulsion, dispersion, precipitation and suspension polymerisation.<sup>17</sup> The continuous phase for heterogeneous CLRP is typically water, but there exists a significant body of work using organic solvents and supercritical CO<sub>2</sub><sup>14, 15</sup>, respectively, as well as various inverse systems where the continuous phase is a non-polar organic solvent and the dispersed phase is aqueous.<sup>53-55</sup> It was proposed early on that of all the dispersed phase polymerisation techniques, miniemulsion polymerisation<sup>3, 4, 56</sup> is most suitable for implementation of the CLRP mechanism. The reason for this is that in a miniemulsion polymerisation, polymer particles are generated directly from pre-formed submicron-size monomer droplets, thus circumventing the issue of phase transfer of the CLRP agent (nitroxide, RAFT agent, Cu(II) complex etc.) through the aqueous phase. However, for CLRP in miniemulsion, one of the main issues initially encountered was superswelling<sup>57</sup>, which leads to colloidal instability and phase separation, particularly in the case of RAFT-controlled polymerisations. This issue can be overcome by careful choice of polymerisation conditions.<sup>58</sup>

The major process drawback of miniemulsion polymerisation is the associated high energy input required to prepare the initial miniemulsion (although low energy systems have been reported<sup>59-61</sup>), and as such it is more industrially-viable to conduct CLRP in an *ab initio* emulsion. However, in an *ab initio* emulsion polymerisation, the control agent must diffuse from the monomer phase (micron-size droplets) through the aqueous phase to reach the main polymerisation locus of the polymer particle. When implementing CLRP into *ab initio* emulsion polymerisation systems, it is essential to avoid monomer droplet nucleation by careful selection of the control agent,<sup>62</sup> otherwise poor control/livingness as well as colloidal instability

result. Typically, this is achieved by avoiding the presence of monomer droplets during the nucleation stage by use of monomer feed techniques, or a pre-synthesised amphiphilic macro-RAFT that initially forms micelles.<sup>17</sup> Several recent papers report successful results using a batch process with amphiphilic macro-RAFT agents formed *in situ* in the presence of monomer droplets.<sup>63-66</sup> In particular, the development of systems where the nucleation step is based on self-assembly of block copolymers<sup>67-71</sup> require no low molecular weight surfactant, as that function is fulfilled by the amphiphilic block copolymer.

Phase transfer (as touched upon above) and partitioning of the CLRP agent can also cause problems for CLRP in dispersed systems. Although phase transfer is not an issue in miniemulsions, partitioning must be considered – for example, if the ligand is too hydrophilic in miniemulsion ATRP, the Cu(II) complex will partition extensively to the aqueous phase, leading to poor control/livingness.<sup>72,73</sup> An intrinsic feature of all CLRP in dispersed systems is the fact that within small particle sizes, such as in microemulsions, there can be an intrinsic broadening effect on the molecular weight distribution due to a statistical variation in the number of control agents between particles.<sup>74</sup> This is closely related to the phenomenon of compartmentalisation,<sup>75,76</sup> which refers to the physical confinement of reactants to nano-size spaces, and is typically observed for particles with  $d < 100$  nm. Compartmentalisation can cause problems depending on the specific conditions/system, but may also lead to improvements in both control and livingness. In some cases, there can also be effects of the oil-water interface on the polymerisation, as specifically reported for NMP.<sup>77,78</sup>

Dispersion polymerisation is often the method of choice when narrow particle size distributions are of importance. For narrow particle size distributions to be obtained, it is a requirement that the particle nucleation stage is completed at low conversion. However, the nucleation stage is prolonged in dispersion CLRP because high molecular weight polymer (which precipitates and leads to particle formation) is not formed instantaneously as in a non-CLRP system, thus yielding broad particle size distributions. This problem can be overcome by use of the so called “two-stage” approach, whereby the control agent (e.g. RAFT agent) is added once the nucleation step has been completed (after a few percent monomer conversion).<sup>79</sup>

We split the review into sections detailing heterogeneous synthesis of block copolymers with different block solubility characteristics: where two or more of the blocks are insoluble in the continuous phase, termed *solvophobic* block copolymer synthesis; or where one or more

blocks are soluble in the continuous phase, termed *amphiphilic* block copolymer synthesis. These two processes are related in some mechanistic details, and have common strategies involved to ensure successful CLRP. However, the *in situ* block copolymer self-assembly processes taking place fundamentally differ, as do the size, structure, properties and potential applications of resulting particulate materials. Within particles comprising two or more blocks that are insoluble in the continuous phase, self-assembly is driven by polymer-polymer phase separation, leading to nanostructured particles of varying morphologies (Fig. 1). These systems will be reviewed in Section 2. In amphiphilic block copolymer synthesis, polymerisation-induced self-assembly (PISA)<sup>80-84</sup> occurs, driven by the different solubility of the blocks in the continuous phase, leading to a range of nano-objects such as spherical micelles, cylindrical micelles, and vesicles (Fig. 2). PISA is an extension of *ab initio* emulsion (and more recently dispersion) CLRP in which synthesis and self-assembly of amphiphilic diblock copolymers takes place *in situ*.<sup>67-69</sup> This body of work will be reviewed in Section 3.

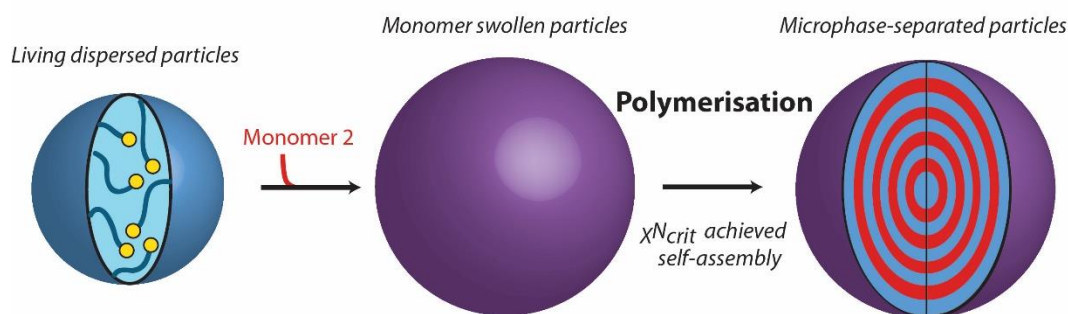


**Figure 1:** Schematic of a solvophobic block copolymer synthesis, in which two or more blocks are insoluble in the continuous phase. The scheme depicts polymer-polymer microphase separation taking place within block copolymer particles during polymerisation, above the critical parameters for phase separation ( $\chi N_{crit}$ , see section 2e for further discussion).

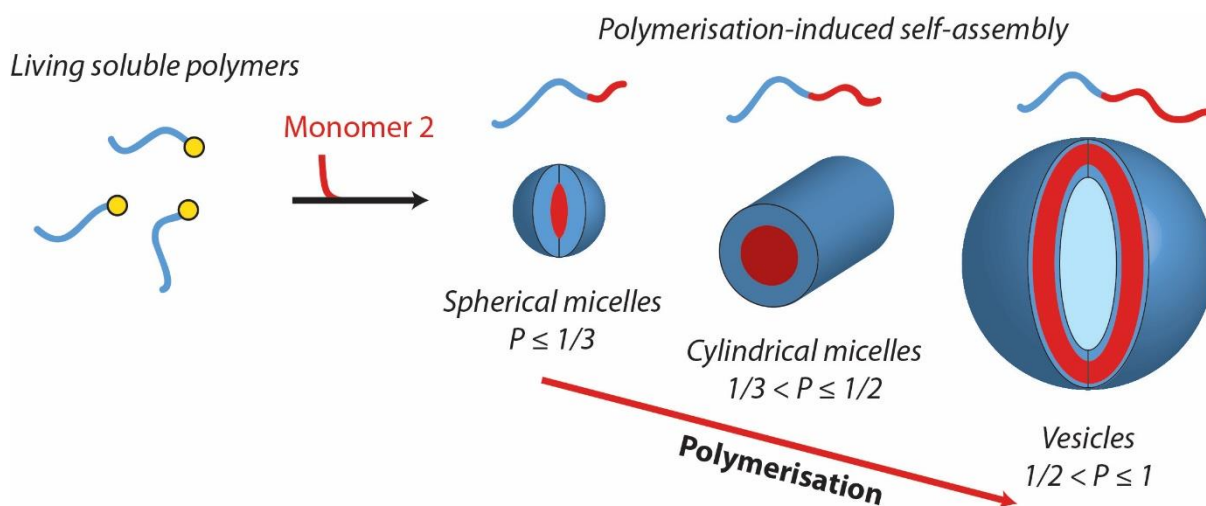


**Figure 2:** Schematic of the polymerisation-induced self-assembly (PISA) of amphiphilic block copolymers upon polymerisation in a selective solvent. The final morphology depends on numerous parameters, primarily the relative lengths of the solvophilic and solvophobic blocks, which can be quantitatively estimated through the packing parameter,  $P = v/al$ , where  $v$  is the volume of the hydrophobic block and  $l$  its length, and  $a$  is the effective interfacial area of the block junction.

## 2. Synthesis and self-assembly of solvophobic block copolymers

As outlined in Section 1b, polymerisation in heterogeneous media maintains low viscosity and good heat transfer throughout the polymerisation, such that sequential monomer addition can be employed in one pot without purification steps: a truly advantageous aspect for block copolymer synthesis over solution or bulk processes. The solvophobic route can produce block copolymer particles with sizes ranging from 50 nm to 10  $\mu\text{m}$ , usually much larger than the length scale of a single block copolymer chain, and within which microphase separation can occur (see discussion in Section 2e) leading to unique material properties and potentially diverse applications. There are examples employing anionic dispersion polymerisation for the synthesis block copolymers using alkanes as the continuous phase,<sup>85, 86</sup> but we focus on the studies adopting ATRP (and its analogues), RAFT/xanthate, NMP, and other CLRP methods, which primarily use water or supercritical  $\text{CO}_2$  ( $\text{scCO}_2$ ) as the continuous phase.

Although a one-pot CLRP reaction is highly coveted from an industrial perspective, there are three main mechanistic limitations (Fig. 3): (1) The pseudo-living nature of CLRP affords block copolymers with a greater *dispersity of chain lengths* (“ $\bar{D}$ ”) relative to traditional

anionic routes; (2) radical-radical termination and chain transfer processes lead to the formation of dead chains or initiation of new polymer chains that are not incorporated into the block copolymer, which leads to loss of “*blocking efficiency*”; (3) unreacted monomers remaining at each step copolymerise with subsequently added monomers, leading to *block sequence impurity*.  $\bar{D}$  is determined by Gel Permeation Chromatography (GPC) and block purity can be quantified through nuclear magnetic resonance (NMR) analysis, whilst there are numerous chromatographic methods for quantifying blocking efficiency (which is usually defined as the percentage of block copolymer chains against the total number of the polymer chains). These include dual detection modes during GPC analysis (Fig. 4A), deconvolution and integration of different populations of chains in GPC traces (Fig. 4B), and HPLC-based separations (gradient polymer elution chromatography (GPEC) and Liquid Adsorption Chromatography (LAC), Fig 4C). In the former, one block is invisible to the UV detector at a particular wavelength (e.g. polybutadiene in polystyrene-block-polybutadiene, PSt-b-PBd), such that only the block copolymer PSt-b-PBd is detected, while both PSt-b-PBd and homo-PS are detected by refractive index (RI). The area of the UV peak relative to the RI peak in the number distribution plots (number of chains vs molecular weight) can then be used to estimate the blocking efficiency in terms of the number fraction (not mass fraction) of living chains.<sup>87</sup> In addition, 2-dimensional approaches coupling LC and GPC have been developed as methods of detecting different homopolymer and block copolymer species.<sup>88</sup> Each method has its own assumptions and drawbacks,<sup>89</sup> and although we report values obtained from the different techniques in this review, quantitative comparison between different studies should be treated with caution. It is widely accepted that there is an intrinsic trade-off between the 3 types of purity from a one-pot process, since reaching a higher conversion of monomer to increase *block sequence purity* leads to an increased propensity of the propagating radicals to undergo termination or chain transfer reactions that lead to an *increase in dispersity*, the loss of livingness, and a lowering of *blocking efficiency*.

In this section, we review the range of conditions and techniques employed in solvophobic block copolymer syntheses with a particular focus on strategies that maximise purity (Sections 2a-2d), followed by a discussion of the consequences of impurities on resulting block copolymer properties and applications (Section 2e). Table 1 summarises some experimental results from the key papers in which block copolymers were synthesised under solvophobic conditions using CLRP methods, mostly in one-pot procedures. As in the table, we will split the discussion by method of CLRP whilst drawing comparisons along the way.

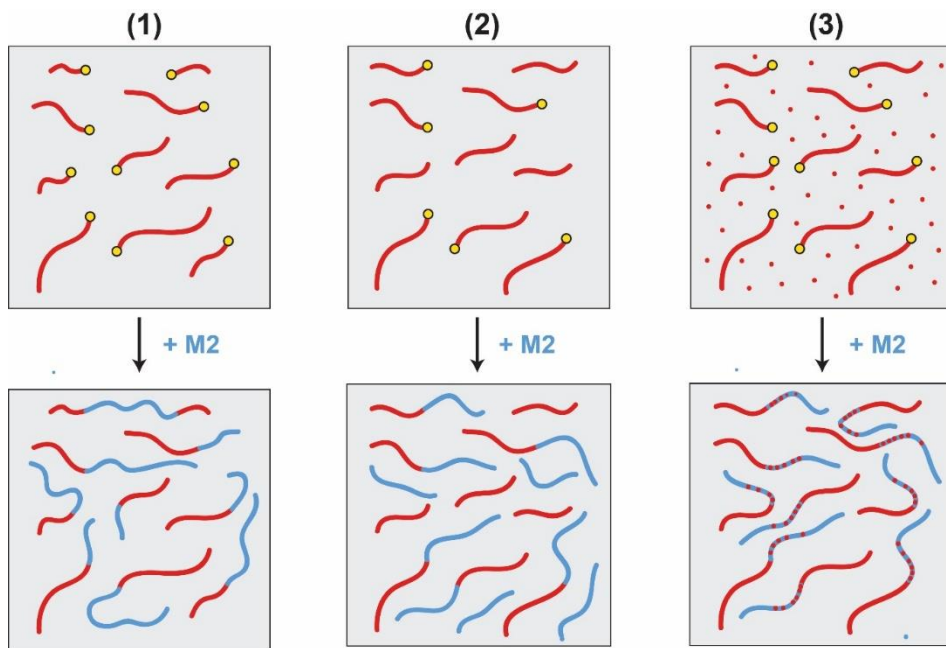


**Figure 3:** Schematic depicting impurities that can arise from one-pot CLRP diblock copolymer synthesis, in which second monomer (M2) addition takes place *in situ*: (1) a *dispersity of chain lengths* ( $\mathfrak{D}$ ) caused by inhomogeneous chain growth and radical side reactions, (2) loss of chain-end functionality, and growth of new chains leading to *low blocking efficiency* and (3) the presence of unreacted first monomer resulting in *block sequence impurity* in the second block. The yellow circles depict the living chain end afforded by CLRP techniques, which should be present in the final block copolymer, but are omitted for clarity.

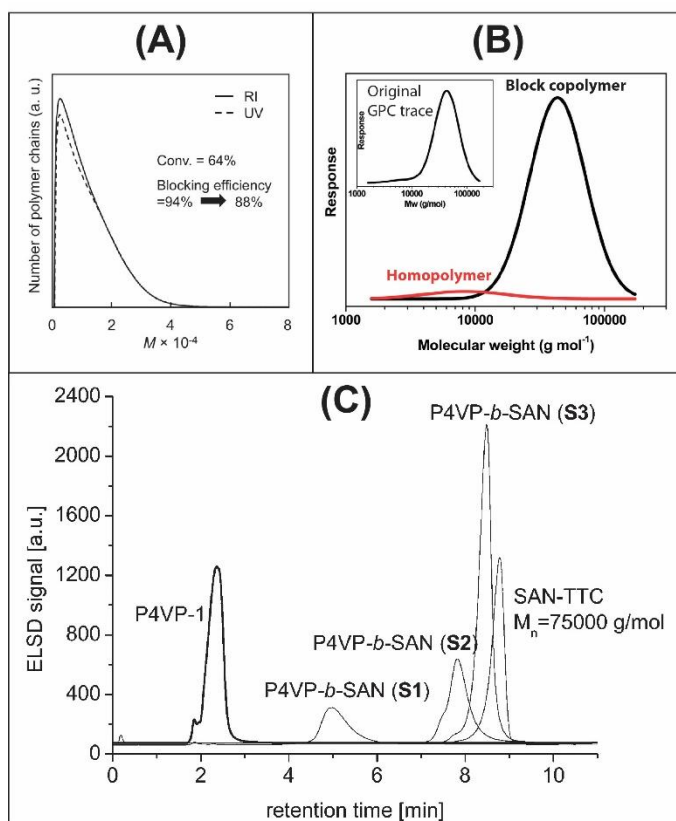


**Figure 4:** Exemplary data from the most common chromatographic methods used to determine blocking efficiency: (A) GPC dual detection, where only the block copolymer is visible by UV detection, while both the block copolymer and homopolymer are visible by RI detection (reproduced with permission from reference<sup>87</sup>, copyright RSC, 2012); (B) GPC deconvolution, in which the GPC trace is split into multiple peaks comprising homopolymer and copolymer (adapted with permission from reference<sup>90</sup>, copyright RSC, 2014); and (C) HPLC, GPEC or LAC, in which homopolymers and copolymer are separated based on their different retention times in gradient solvent mixtures (reproduced with permission from reference<sup>91</sup>, copyright ACS, 2007).

**Table 1:** Summary of conditions adopted for block copolymer syntheses conducted by CLRP under solvophobic conditions and resulting polymer characteristics.

Block copolymer	Heterogeneous system	CLRP method	Monomer Cv % (step 1, step 2 etc.)	Final MW /kg mol <sup>-1</sup>	Final D	Blockin g efficiency	Dispersant	ref
P <sup>n</sup> BuA-b-PSt	Microemulsion/ab initio	AGET ATRP	50, 63	26	1.3	n/r	Brij 98	92
P <sup>i</sup> BMA-b-PSt	Miniemulsion + seeded	ATRP	99, 40	30	1.1	n/r	Tween 80	93
P <sup>i</sup> BMA-b-PSt	Miniemulsion + seeded	ATRP	97, 90	52	1.26	n/r	Tween 80	94
P <sup>i</sup> BMA-b-PSt	Microsuspension	AGET ATRP	71, 94	76	2.4	61	Brij 98	95
P <sup>i</sup> BMA-b-PSt	Microsuspension	AGET ATRP	80, 95	75	2.4	62	Brij 98	96
PFMA-b-PSt	Microemulsion	AGET ATRP	89, 73	14	1.19	n/r	OP-10	97
PSt-b-P <sup>n</sup> BuA-b-PSt	Ab initio emulsion	AGET ATRP	~50, n/r	74	2.8	n/r	CTAB	98
PSt-b-P <sup>n</sup> HA-b-PSt	Ab initio emulsion	AGET ATRP	~50, n/r	45	2.0	n/r	CTAB	98
POEG <sub>300</sub> MA-b-POEG <sub>475</sub> MA	Miniemulsion <sup>x</sup>	AGET ATRP	n/r, 85	69	1.30	n/r	Span 80	99
PMMA-b-PFMA	Dispersion*	ATRP	90, 32	65	1.40	n/r	PFMA-co-TEDETA	100
PAA-b-PSt	Precipitation*	ATRP	86, 60	68	8.21	25	None	101
PSt-b-(PBuA-co-PAAEMA)	Ab initio emulsion	RAFT	>95, n/r	n/r	n/r	76	SDS	89
PBuA-b-PSt	Ab initio emulsion	RAFT	>95, >95	n/r	n/r	90	SDS	102
PSt-b-P <sup>n</sup> BuA	Seeded emulsion	RAFT	96, >95	20	1.3	90	SDS	103
PSt-b-P <sup>n</sup> BuA	Microemulsion	RAFT	95, 96	99	2.02	n/r	SDS	104
PSt-b-P <sup>n</sup> BuA	Miniemulsion	RAFT	80, n/r	40	1.7	n/r	SDS	105
PSt-b-PBuA	Miniemulsion	RAFT	90, 80	80	2.16	n/r	Igapol® CO-990	106
PBuA-b-PSt	Miniemulsion	RAFT	88, 88	100	2.07	n/r	Brij 98®	106
PSt-b-P <sup>n</sup> BuA-b-PSt	Ab initio emulsion	RAFT	92,95,96	131	2.36	>90 <sup>‡</sup>	PAA-b-PSt-TTC	107
PSt-b-P <sup>n</sup> BuA	Ab initio emulsion	RAFT	n/r, 91	139	2.17	>90 <sup>‡</sup>	PAA-b-PSt-TTC	107
PSt-b-P <sup>n</sup> BuA-b-PSt	Ab initio emulsion	RAFT	95, 95, 97	95	1.54	n/r	PAA-b-PSt-TTC	108
PSt-grad-P <sup>n</sup> BuA	Ab initio emulsion	RAFT	98, 97	91	1.58	>89 <sup>‡</sup>	PAA-b-PSt-TTC	109
PSt-b-P <sup>n</sup> BuA-b-PSt	Miniemulsion	RAFT	>95, >95	81	2.49	n/r	PSt-b-PMA-DTB	110
P <sup>n</sup> BuA-b-PSt	Miniemulsion	RAFT	>98, 97	75	2.0	n/r	SDS	111
PVDC-b-PSt	Ab initio emulsion	RAFT	78, n/r	76	1.6	n/r	PAA-b-PSt-TTC	112
PSt-b-PBd	Miniemulsion	RAFT	81, 24	63	2.84	>95 <sup>‡</sup>	SDS	113
PBd-b-PSt	Ab initio emulsion	RAFT	76, 71	26	1.62	n/r	PAA-b-PSt-TTC	114
PSt-b-PBd-b-PSt	Miniemulsion	RAFT	80, 30,30	90	2.73	>90 <sup>‡</sup>	SDS	115
PSt-b-(PSt-co-PBd)-b-PBd	Miniemulsion	RAFT	53, 73	77	2.7	>>95	Potassium oleate	116
PMMA-b-P <sup>n</sup> BuA	Ab initio emulsion	RAFT	97, 100	116	3.26	n/r	PMAA-b-PMMA-TTC	117
PDMA-b-PDEA	Microemulsion <sup>†</sup>	RAFT	95, 54	13	1.07	n/r	POE(6)C18	118



PMMA-b-P4VP	Dispersion*	RAFT	>90, >90	68	1.98	n/r	PDMS-MA	119
PMMA-b-PDMAEMA	Dispersion*	RAFT	>90, 86	44	1.33	n/r	PDMS-MA	119
PMMA-b-PDMA	Dispersion*	RAFT	>90, >90	94	1.69	n/r	PDMS-MA	119
PMMA-b-PSt	Dispersion*	RAFT	>98, >90	55	1.40	57	PDMS-MA	120
PMMA-b-PBzMA	Dispersion*	RAFT	>98, >90	92	1.24	76	PDMS-MA	120
PEEMA-b-PDMA	Seeded precipitation*	RAFT	n/r, 40	15	1.27	n/r	None	121
PEEMA-b-P4AM	Seeded precipitation*	RAFT	n/r, 87	35	1.35	n/r	None	121
PSt-b-P <sup>n</sup> BuA-b-PSt	Miniemulsion	NMP	89, 90	59	3.95	n/r	Dowfax 8390	122
PSt-b-P <sup>n</sup> BuA-b-PSt	Ab initio emulsion	NMP	71, 85	51	1.64	>99	Dowfax 8390	122
PMMA-b-P <sup>n</sup> BuA-b-PMMA	Ab initio emulsion	NMP	60, 45	143	2.00	>95	Dowfax 8390	122
PSt-b-P <sup>n</sup> BuA	Continuous miniemulsion	NMP	99, 92	39	2.02	n/r	SDBS	123
PSt-b-P <sup>n</sup> BuA-b-PSt	Continuous miniemulsion	NMP	99, 80, 90	58	2.30	n/r	SDBS	123
PDMA-b-PNIPAM	Precipitation/suspension*	NMP	n/r	31	1.63	n/r	none	124
P <sup>n</sup> BuA-b-PNIPAM	Precipitation/suspension*	NMP	n/r	35	1.31	n/r	none	124
PSt-b-PNIPAM	Precipitation/suspension*	NMP	24, 51	31	1.63	n/r	none	124
PMMA-b-PBzMA	Miniemulsion	RTCP	64, 64	12	1.4	88	TTAB	87
P <sup>n</sup> BuA-b-P <sup>n</sup> BuA	Suspension	Fe(II)	94, 92	25	1.41	n/r	None	125
P <sup>n</sup> BuA-b-PSt	Suspension	Fe(II)	92, 80	28	1.22	n/r	None	125
P <sup>n</sup> BuA-b-PSt	Suspension	Fe(II)	97, 63	35	1.40	n/r	None	125
P <sup>n</sup> BuA-b-PSt	Ab initio emulsion	RITP	75, 52	16	1.8	n/r	SHS	126
P <sup>n</sup> BuA-b-PSt	Ab initio emulsion	TERP	80, n/r	140	1.74	76	PMAA-TeMe	127
PSt-b-PMMA	Dispersion*	RTCP	n/r, 70	12.5	2.05	75	PDMS-Azo	128
<b>PVAc-b-PAN</b>	<b>Precipitation/dispersion*</b>	<b>CMRP</b>	<b>13, 77</b>	<b>48</b>	<b>2.01</b>	<b>n/r</b>	<b>None</b>	129

All polymerisations conducted with an aqueous medium as the continuous phase, except where specified; n/r = value not reported; \*polymerisation conducted in scCO<sub>2</sub>; †polymerisation conducted in hexanes; ‡polymerisation conducted in cyclohexane; †blocking efficiency value not measured experimentally but estimated based on calculated proportion of living chains (see section 2b).

## 2.a. ATRP

Min *et al.* were the first to employ Activators Generated by Electron Transfer (AGET) ATRP for the synthesis of poly(n-butyl acrylate)-b-polystyrene (P<sup>n</sup>BuA-b-PSt) in a two-step *ab initio* emulsion.<sup>92</sup> A small quantity of <sup>n</sup>BuA, ATRP initiator and catalyst were first formed into microemulsion micelles, and after initiation further <sup>n</sup>BuA was added to form droplets and set up a traditional emulsion system. This strategy ensured that catalyst remained at the locus of polymerisation within micelles (i.e. partitioning across the aqueous phase into monomer droplets was minimised), and enabled the <sup>n</sup>BuA polymerisation to proceed with controlled kinetics. After *in situ* St addition and resumption of polymerisation, a block copolymer with low Đ (1.3) and a high blocking efficiency (not quantified) was obtained. However, St was added after low conversion of <sup>n</sup>BuA (50%), leading to low PSt block sequence purity since <sup>n</sup>BuA and St formed a random copolymer. The group also had success in emulsion-based block copolymer synthesis by preparing a macroinitiator in bulk polymerisation and chain extending in dispersed conditions, but these multistep procedures will not be discussed here.<sup>130, 131</sup>

The Okubo group published multiple reports on poly(iso-butyl methacrylate)-b-PSt (P<sup>i</sup>BuMA-b-PSt) synthesis using various forms of ATRP in aqueous emulsion.<sup>93-96</sup> In their first report, P<sup>i</sup>BuMA synthesis was controlled using copper bromide in a miniemulsion polymerisation, before an emulsion of St was added to afford a seeded mechanism by swelling of the particles generated in the first step.<sup>93</sup> The P<sup>i</sup>BuMA-b-PSt MW agreed well with the expected value, Đ was low (1.1) and blocking efficiency thought to be high based on qualitative thin layer chromatography (TLC) analysis, but St conversion was low (40%). This issue was addressed in their following study by optimising emulsifier (Tween 80) concentration used during <sup>i</sup>BuMA polymerisation.<sup>94</sup> At lower emulsifier concentration, large particles formed as a result of coagulation, which led to poor monomer absorption into particles and low conversion, whilst at high emulsifier concentration, the large interfacial area lead to escape of copper-ligand complexes from the particles and low conversion. At an optimum 6-10 wt% emulsifier concentration range, St conversion was high (>80%) whilst Đ remained low (ca. 1.25). However, the slow St propagation by the ATRP route required excessive reaction time, which was later addressed by adopting AGET ATRP miniemulsion.<sup>95</sup> St polymerisation rate was significantly enhanced in miniemulsion conditions, but block copolymer Đ was high (2.4) due to a significant quantity of homo-P<sup>i</sup>BuMA and low blocking efficiency (<50%). By measuring the fraction of living chains at different stages of polymerisation (using a GPC dual detection method), it became evident that a significant quantity of dead chains formed during the early

stages of St polymerisation. Blocking efficiency was improved by reducing the ascorbic acid concentration (which lowers radical concentration), and introducing St as an aqueous emulsion rather than the monomer alone. In addition, the mixture of P<sup>i</sup>BuMA seed and St was stirred at 40 °C prior to heating to the final polymerisation temperature (70 °C), which was thought to expedite the reinitiation step and lower the radical concentration in the early stage of polymerisation. Integrating these steps increased the blocking efficiency to 61%, although St was added after 71% <sup>i</sup>BuMA conversion, effecting low block sequence purity. The effect of St polymerisation temperature on blocking efficiency in P<sup>i</sup>BuMA-b-PSt was studied in a follow-up report,<sup>96</sup> with values of 62, 58 and 51% resulting from 70, 90 and 110 °C, respectively. A larger proportion of living chains to be reinitiated existed at lower temperature due to a reduced termination rate. This series of studies from the Okubo group highlights that the conditions during chain extension of the first block can influence blocking efficiency. Shu et al. also adopted AGET ATRP with an aqueous continuous phase, to synthesise partially fluorinated copolymers including poly(2,2,2-trifluoroethyl methacrylate-b-PSt (PFMA-b-PSt).<sup>97</sup> Fluorinated monomers were polymerised in a microemulsion stabilised by an anionic surface-active AGET ATRP initiator and chain extension with St took place *in situ*. The resulting block copolymers had low Đ (>1.15) and high block sequence purity (St added at 89% FMA conversion). The high purity copolymer, superior to the above results by the Okubo group, may be a result of the surface-active AGET ATRP initiator, or the use of a microemulsion system.

A rigorous study into a range of ligands and surfactants for AGET ATRP was performed by Xue et al for the synthesis of PSt-b-P<sup>n</sup>BuA-b-PSt using a difunctional ATRP initiator.<sup>98</sup> The authors concluded that the most hydrophobic ligand (BPMODA), which partitioned less into the aqueous phase, controlled polymerisation best (lower Đ). The surfactant cetyltrimethylammonium bromide (CTAB) provided optimal colloidal stability without interfering with polymerisation control due to its superior stability at higher temperature. The group also found that control over n-hexyl acrylate (<sup>n</sup>HA) exceeded <sup>n</sup>BuA, which was again ascribed to lower partitioning to the aqueous phase of the more hydrophobic monomer.

There are also reports of ATRP-controlled solvophobic block copolymer synthesis in non-aqueous solvents. The research group of Matyjaszewski prepared POEG<sub>300</sub>MA-b-POEG<sub>475</sub>MA (where OEG<sub>x</sub>MA is oligoethylene glycol methacrylate with monomer molar mass of x) controlled by AGET ATRP in an inverse miniemulsion in cyclohexane at ambient temperature (30 °C).<sup>99</sup> PEG-Br or PEG-OH (end-functional polyethylene glycols) acted as cosurfactants to facilitate control over MW and colloidal stability during polymerisation, and well-controlled

( $\bar{D} < 1.3$ ) hydrophilic block copolymer particles were obtained. However, the synthesis was not conducted in one pot, as POEG<sub>300</sub>MA was synthesised within an inverse emulsion, then purified and re-emulsified in the presence of OEG<sub>475</sub>MA prior to chain extension.

Grignard *et al.* adopted scCO<sub>2</sub> as the medium for AGET ATRP-controlled synthesis of partially-fluorinated block copolymer poly(methyl methacrylate)-block-PFMA (PMMA-*b*-PFMA).<sup>100</sup> The dispersion polymerisation was stabilised by a fluorinated polyacrylate containing triamine comonomer units (tetraethyldiethylenetriamine, TEDETA), which ligated copper and enhanced the catalyst concentration at the polymerisation locus. With an optimal number of TEDETA-functional units in the stabiliser (3), simultaneous control over polymerisation kinetics and stabilisation of a PMMA dispersion was achieved. After addition of FMA at high pressure and resumption of polymerisation, the resulting block copolymer possessed low  $\bar{D}$  (1.4). However, blocking efficiency was fairly low (as indicated by a low MW homo-PMMA shoulder in the GPC trace), and the final MW deviated from the targeted value in both PMMA and PMMA-*b*-PFMA, hinting that control and livingness were lower than in RAFT-controlled block copolymer synthesis in scCO<sub>2</sub> dispersion (*vide infra*). Minami *et al.* also used scCO<sub>2</sub>, as a medium for reverse ATRP synthesis of poly(acrylic acid)-*b*-PSt (PAA-*b*-PSt) in a precipitation polymerisation. This system enabled the use of a less air sensitive copper (II) complex that was reduced by initiator to the corresponding copper (I) complex.<sup>101</sup> The non-linear polymerisation kinetics and high  $\bar{D}$  PAA (2) strongly suggested an uncontrolled process. After depressurisation of the reactor, St was added and polymerised by a seeded direct ATRP mechanism under scCO<sub>2</sub> conditions. Block copolymer formation was evidenced by an increase in molecular weight, but  $\bar{D}$  was very high (8.2, analysed after methylation), and blocking efficiency estimated to be 25%. The amphiphilic structure of the block copolymer was demonstrated by emulsifying oil in water, which suggests that even these very low purity block copolymers can yield useable materials.

## 2.b. RAFT

In contrast to ATRP, RAFT proceeds *via* a degenerative transfer mechanism in which the chain transfer agent (CTA) remains chemically bound to the growing polymer chain throughout the polymerisation, thus potentially minimising detrimental effects of reagent partitioning. This may explain why, to date, solvophobic block copolymer syntheses under RAFT control are most numerous. The majority of these studies have focussed on the synthesis of <sup>n</sup>BuA-St

copolymers in aqueous conditions, although the recent expansion to non-aqueous systems (hexanes, supercritical CO<sub>2</sub>) has widened the range of polymers accessible by solvophobic RAFT-controlled synthesis.

Monteiro and coworkers pioneered solvophobic synthesis of block copolymers under aqueous emulsion conditions, using low reactivity xanthates as control agents for the P<sup>n</sup>BuA-b-PSt system.<sup>89, 102-104</sup> In their first study,<sup>102</sup> P<sup>n</sup>BuA latexes with controlled MW and fairly low Đ (1.6) were synthesised to high monomer conversion (95%) and swollen with an aliquot of St overnight before polymerisation was reinitiated. The swelling step ensured time for diffusion and homogeneous distribution of St throughout the P<sup>n</sup>BuA latex. The remaining volume of St was added either in one batch or as a “starved feed” at a rate of 0.2 ml min<sup>-1</sup>, after which resulting blocking efficiency was measured to be 70 or 90%, respectively (determined by GPC dual detection). Following this, the group synthesised PSt-b-(PBuA-co-PAAEMA), (where PAAEMA is polyacetoacetoxyethyl methacrylate) in an *ab initio* emulsion.<sup>89</sup> BuA and PAAEMA were introduced to PSt particles as a pre-formed miniemulsion under batch or starved feed conditions, which led to 65 and 76% blocking efficiency, respectively (as analysed by GPEC). These dramatic differences in the blocking efficiency between batch and starved-feed conditions were attributed to lower radical entry efficiency into particles during starved-feed, leading to fewer terminations and a greater proportion of living chains,<sup>102</sup> and/or the formation of more secondary particles under batch conditions.<sup>89</sup> In a follow up study, the authors reversed the block order and employed PMMA particles (d = 57 nm) to seed the polymerisation of St, which overcame the colloidal instability of the *ab initio* emulsion and improved control over the particle size distribution.<sup>103</sup> After synthesis of a PSt block with high dispersity (Đ = 2, which was predicted for this xanthate-controlled St polymerisation), unreacted St was extracted by dialysis and the particles were swollen overnight with a portion of <sup>n</sup>BuA. The remaining <sup>n</sup>BuA was added by starved-feed at variable feed rates, and it was found that block copolymer Đ decreased as feed rate decreased, to a minimum of ~1.3. High blocking efficiency (>90%, determined by HPLC) was reported at low feed rate, even after high St conversion (96%). The studies conducted by the Monteiro group emphasised that processing conditions can be tailored to enhance control over polymerisation: simply lowering the second monomer feed rate encourages simultaneous growth of all polymer chains. The amphiphilic character of the xanthate CTAs was also reasoned to be beneficial to the control and high blocking efficiency in these studies, reaffirming that CTA solubility is a non-trivial matter in solvophobic block copolymer synthesis.

An industrially-attractive continuous miniemulsion was employed by Smulders *et al.* for synthesis of PSt-*b*-P<sup>n</sup>BuA using a dithiocarbonate RAFT agent.<sup>105</sup> By employing continuous stirred tank reactors, and beginning with a St miniemulsion, flow rates between reactors could be controlled in order to synthesise sophisticated polymers with multiple random copolymer (PSt-co-P<sup>n</sup>BuA) blocks of variable composition. Residence times within the 4 reactors were varied in order to control the conversion of St before addition to a <sup>n</sup>BuA macroemulsion. Initial experiments afforded block copolymers with bimodal molecular weight distribution (MWD), but lower Đ (down to 1.7) was achieved by taking St polymerisation to higher conversion (up to 80%). The bimodal traces were attributed to secondary nucleation of <sup>n</sup>BuA particles and subsequent polymerisation controlled by unreacted RAFT agent. This study hints at another detrimental factor of unreacted monomer, not only in affecting the block sequence purity, but also potentially the overall colloidal stability within the process.

A study by Bowes and coworkers highlighted the importance of monomer polymerisation order and RAFT agent functionality under aqueous miniemulsion conditions, by comparing synthesis of P<sup>n</sup>BuA-*b*-PSt, PSt-*b*-P<sup>n</sup>BuA and ABA triblock analogues (from the analogous difunctional trithiocarbonates).<sup>106</sup> In all cases, living chain growth was observed in the first step, but deviations from theoretical MW were observed upon chain extension, and final block copolymer Đ was high (2-2.5). Notably, blocking efficiency (measured by GPC dual detection) was higher in P<sup>n</sup>BuA-*b*-PSt than PSt-*b*-P<sup>n</sup>BuA. The authors proposed that the slower nucleation of PSt resulted in lower livingness than P<sup>n</sup>BuA, even though the polystyryl radical is a better leaving group from a trithiocarbonate RAFT agent than the polyacrylate radical, which suggests that a compromise between radical chemistry and colloidal stability must be considered when selecting the order of polymerisation. Furthermore, higher Đ and lower blocking efficiency were found in both ABA copolymers synthesised from a difunctional RAFT agent, which was attributed to a mixture of polymers containing one or two RAFT functionalities resulting from the first step of polymerisation.

There are a number of reports adopting continuous phase-soluble polymeric CTAs for RAFT-controlled solvophobic block copolymer synthesis. The research group of Hawlett employed a hydrophilic macro-RAFT agent (trithiocarbonate-functional PAA, PAA-TTC) to overcome the earlier-discussed issues associated with particle nucleation in the *ab initio* emulsion synthesis of P<sup>n</sup>BuA-*b*-PSt.<sup>132</sup> After achieving >99% <sup>n</sup>BuA conversion, chain extension with St led to block copolymer with qualitatively high blocking efficiency. Following this, a short <sup>n</sup>BuA or St block was included in the macro-RAFT agent to introduce

amphiphilicity into the CTA and to prevent the initial formation of droplets.<sup>133</sup> The group prepared PAA-b-P<sup>n</sup>BuA-b-PSt-b-P<sup>n</sup>BuA and PAA-b-PSt-b-P(<sup>n</sup>BuA-co-MMA) from PAA-b-P<sup>n</sup>BuA-TTC and PAA-b-PSt-TTC macro-RAFT agents, respectively, although no macromolecular characterisation was provided to compare to their earlier study. Luo *et al.* also adopted PAA-b-PSt-TTC as a macro-RAFT agent and surfactant in a sequential aqueous emulsion route to PSt-b-P<sup>n</sup>BuA-b-PSt (SBAS).<sup>107</sup> The controlled synthesis of PSt resulted in lower  $\bar{D}$  (1.2-1.5) than in the RAFT studies discussed above, suggesting that colloidal instability and nucleation issues were minimised by using an amphiphilic macro-RAFT agent.  $\bar{D}$  increased significantly (up to 3) upon polymerisation of <sup>n</sup>BuA, which was ascribed to the onset of phase separation within the particles, attendant with a lower mobility and chain transfer constant of the polymeric RAFT agent. Despite this high  $\bar{D}$ , controlled polymerisation was resumed upon addition of further St to afford SBAS copolymers with  $\bar{D}$  mostly >2 (and dependent on total molecular weight). Each block proceeded to high conversion (>90%), and the authors estimated a high blocking efficiency (>93% by theoretical calculation), which was qualitatively supported by GPC dual detection analysis. In a following study, the factors leading to large  $\bar{D}$  values in SBAS were investigated.<sup>108</sup> Decreasing the charge on the PAA segment of the macro-RAFT agent led to lower block copolymer  $\bar{D}$  (down to 1.4), which was attributed to a higher entry efficiency of radicals from the aqueous phase increasing termination of midchain radicals that would otherwise lead to branches. The Luo research group expanded on the amphiphilic macro-RAFT agent strategy to synthesise gradient SBAS copolymers using a “many-shot” approach.<sup>109</sup> After polymerisation of the initial St emulsion, 8 different ratios of St/<sup>n</sup>BuA were added at different time intervals, with increasing <sup>n</sup>BuA fractions. High monomer conversion (>95%) was allowed before addition of subsequent shots, which afforded PSt-grad-P<sup>n</sup>BuA and PSt-grad-P<sup>n</sup>BuA-grad-PSt copolymers with low  $\bar{D}$  (1.3-1.6) and block-like character. The short reaction times required in each step facilitated high blocking efficiency, with dead chain content theoretically calculated to be ca. 11% after multiple steps.

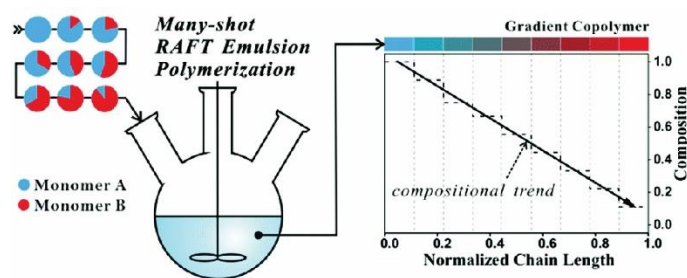


**Figure 5:** Schematic of the “many-shot approach” to the synthesis of gradient copolymers in a one-pot RAFT emulsion polymerisation. Reproduced with permission from reference<sup>109</sup>, copyright RSC, 2014.

Zhan *et al.* used polymeric RAFT agents comprising thio-ester functional hydrophilic St-alt-maleic anhydride (SMA) copolymers to control the synthesis of SBAS under miniemulsion conditions by sequential monomer addition.<sup>110, 134</sup> A dramatic increase in  $\bar{D}$  was observed during <sup>n</sup>BuA polymerisation, and attributed to the increasing viscosity within the particle. The final block copolymer  $\bar{D}$  varied from 2.5 up to 3.75 as a function of SMA-RAFT MW (2 to 15 kg mol<sup>-1</sup>), which was explained by the more embedded RAFT functionality leading to a lower transfer constant and an increased number of dead chains formed (calculated to be <10% at each step). Yang *et al.* exploited both strategies of an amphiphilic polymeric RAFT agent (PDMA-b-(P<sup>n</sup>BuA-co-PGIMA), where GIMA is glycidyl methacrylate) and starved feed addition of monomers in the miniemulsion RAFT synthesis of P<sup>n</sup>BuA-b-PSt.<sup>111</sup> Whilst control over MW was good in all stages,  $\bar{D}$  increased to ca. 2-3 during St polymerisation. The studies also disclosed a significant effect of target molecular weight on purity: much higher  $\bar{D}$  was obtained when targeting higher MW polymers, perhaps an effect of the block copolymer phase separation that was observed within the particles (*vide infra*).

A number of studies have focussed on the synthesis of St-butadiene block copolymers (known as SBS in their triblock form), which are benchmark thermoplastic elastomer materials that are commercially synthesised by solution-phase anionic polymerisation.<sup>135</sup> Wei *et al.* demonstrated aqueous miniemulsion synthesis of PSt-b-PBd controlled by a dithioacetate.<sup>113</sup> After well-controlled St polymerisation, the resulting PSt latex was swollen in Bd for 2 h before polymerisation was resumed. With increasing Bd conversion,  $\bar{D}$  rapidly increased until the polymer became cross-linked, due to the inevitable side reactions of PBd. However, based on the rapid St polymerisation, it was hypothesised that livingness and therefore blocking efficiency would be high (>95%). Later, the authors reversed the block order (PBd-b-PSt) in



*ab initio* emulsion polymerisation, with the aim of averting cross-linking.<sup>114</sup> Using a series of PAA-b-PSt-TTC macro-RAFT agents, it was determined that an optimum PAA length (27 units) provided good colloidal stabilisation whilst minimising the inhibition period in Bd polymerisation. PBd with low MW was targeted to avoid cross-linking, from which chain extension with St afforded reasonably well controlled PAA-b-PSt-b-PBd-b-PSt ( $\bar{D} = 1.62$ ), although GPC data suggested blocking efficiency was not high. Authors from the same group later exploited miniemulsion RAFT to synthesise PSt-b-PBd-b-PSt with high MW (ca. 100 kg mol<sup>-1</sup>), and avoided cross-linking by arresting the Bd polymerisation at 30% conversion.<sup>115</sup> Although they calculated dead chain fraction to be low (>10%), block sequence purity was lower and branching of PBd led to high  $\bar{D}$  (2.7-2.8). Froimowicz *et al.* developed a “non-stop” miniemulsion RAFT route to the triblock PBd-b-PSt-b-PBd from a difunctional trithiocarbonate, thus reducing the number of polymerisation steps.<sup>116</sup> Bd was added before polymerisation of the central St block was complete, and polymerisation immediately resumed. The resulting block copolymers had very high blocking efficiency (no homopolymer detectable by HPLC), but at the expense of low block sequence purity. However, above ~53% St conversion, the presence of homo-PSt became measureable by HPLC. In addition, the authors avoided cross-linking until 70% Bd conversion, which hints at a more controlled polymerisation than by Wei *et al.*,<sup>113</sup> who encountered a gel point at 25% Bd conversion at comparable MW. This may be the result of the trithiocarbonate RAFT agent (which is more commonly employed to control Bd polymerisation than dithioacetates<sup>136</sup>) or the copolymerisation of St and Bd averting cross-linking. A more recent study by Wang *et al.* supports this latter conclusion, where cross-linking was avoided by adding a mixture of St and Bd monomers to a PSt miniemulsion, affording PSt-b-(PSt-co-PBd) copolymer with low  $\bar{D}$  (1.5) from a dithioacetate-controlled process.<sup>137</sup>

Some groups have investigated monomers beyond the most common styrene-butyl acrylate and styrene-butadiene-based polymers. Yang *et al.* prepared the tetrablock copolymer PAA-b-PSt-b-PVDC-b-PSt by chain extending PAA-b-PSt-TTC macro-RAFT with vinylidene chloride (VDC) and St.<sup>112</sup> Deprotonating PAA by adding NaOH during polymerisation of VDC (but not before initiation) was found to be a key step to ensuring emulsion stability and polymerisation control, as it was thought to prevent desorption of initiating radicals. The final block copolymer had fairly low  $\bar{D}$  (1.6), although the appearance of a shoulder in GPC traces hinted at a population of dead polymer chains. Luo *et al.* prepared an all-acrylic poly(methacrylic acid)-b-PMMA-b-P<sup>n</sup>BuA (PMAA-b-PMMA-b-P<sup>n</sup>BuA)<sup>117</sup> by aqueous *ab*

*initio* emulsion polymerisation starting from a PMAA-b-PMMA-TTC macro-RAFT agent. MMA was rapidly polymerised to high conversion, and PMMA  $\bar{D}$  (1.5) was found to be higher than from macro-RAFT agents containing PSt or P<sup>n</sup>BuA blocks in the reports discussed above, which was attributed to a non-uniform distribution of RAFT agents between particles. Block copolymer  $\bar{D}$  was very high (>3.2) due to P<sup>n</sup>BuA branching, but blocking efficiency appeared to be good based on GPC dual detection.

Studies adopting non-aqueous systems for RAFT-controlled synthesis of solvophobic block copolymers are fewer in number, but demonstrate extension of the concept to a wider range of polymer structures. For example, Sogabe *et al.* established an inverse microemulsion route to a dimethyl acrylamide (DMA)-diethylacrylamide (DEAA) triblock copolymer (PDMA-b-PDEAA-b-PDMA) from a difunctional trithiocarbonate in hexanes.<sup>118</sup> A low concentration of dispersed aqueous phase was necessary to achieve good colloidal stability of the initial microemulsion, but this resulted in a long induction period and loss of control. By increasing the number of RAFT agents per particle, low MW copolymer (<20 kg mol<sup>-1</sup>) with high block sequence purity (DMA conversion 95% upon DEAA addition) and very low  $\bar{D}$  (1.07) was produced, but MW deviated from theoretical values, which was explained by partitioning of the RAFT agent.

The research group of Howdle conducted RAFT-controlled block copolymer synthesis in scCO<sub>2</sub> using a CO<sub>2</sub>-soluble trithiocarbonate to synthesise PMMA-b-PSt, PMMA-b-poly(benzyl methacrylate) (PMMA-b-PBzMA), PMMA-b-poly(N,N-dimethylaminoethyl methacrylate) (PMMA-b-PDMAEMA), PMMA-b-poly(4-vinylpyridine) (PMMA-b-P4VP) and PMMA-b-PDMA.<sup>119, 120, 138</sup> PMMA particles were synthesised in a dispersion polymerisation stabilised by monomethacrylate-functional polydimethylsiloxane (PDMS-MA), before the second monomer was added under pressure (with or without additional initiator) and the polymerisation immediately resumed. Block copolymer  $\bar{D}$  was low for PMMA-b-PBzMA and PMMA-b-PDMAEMA (1.2-1.5) but higher for PMMA-b-PSt, PMMA-b-P4VP and PMMA-b-PDMA (1.5-2.5). The latter observation could be explained by the tendency for termination by combination in St, 4VP and DMA polymerisations, resulting in a population of high MW chains. Blocking efficiency was estimated using a number of chromatographic methods, and found to be highly sensitive to RAFT:initiator ratio used in PMMA synthesis, block copolymer target MW and the identity of the second block. With the lowest initiator concentration, and at lower target MW (60 kg mol<sup>-1</sup>), the highest blocking efficiency was obtained for PMMA-b-PBzMA (82%, measured by a combination of GPC and GPEC), which

compared favourably with theoretical calculations based on estimates for the fraction of RAFT-functional PMMA chains.<sup>120</sup> PMMA-*b*-PSt copolymers had lower blocking efficiencies (<59%) due to a significant quantity of homo-PSt chains formed as a result of high initiator concentrations that were adopted in St polymerisations to enable full conversion from the slower propagating monomer. These blocking efficiencies were relatively high, considering the near-quantitative conversion of the PMMA block (>90%) and high block sequence purity (proven by <sup>1</sup>H NMR analysis). The efficiency of the process was attributed to the plasticisation of polymer particles and high diffusivity afforded by scCO<sub>2</sub>, which would facilitate monomer access to the living chain ends. Hawkins *et al.* exploited scCO<sub>2</sub> in a precipitation polymerisation during the second step of block copolymer synthesis.<sup>121</sup> DTB-functional poly(2-ethoxyethyl methacrylate) (PEEMA) was first prepared in solution then dissolved in monomer (DMA or 4-acrylomorpholine, 4AM). CO<sub>2</sub> was added and the mixture heated into the supercritical state, upon which the monomer swollen macro-RAFT particles precipitated from solution and polymerisation began. The resulting block copolymers displayed relatively low  $\bar{D}$  (<1.38), and blocking efficiency was equivalent to when conducting the chain extension in solution. The high pressure of scCO<sub>2</sub> was exploited to flush the reactor post-polymerisation, and as with most optimised syntheses in scCO<sub>2</sub>, polymers were monomer-free powders requiring no further purification.

### 2.c. NMP

The group of Charleux first reported block copolymer synthesis via NMP in aqueous miniemulsion.<sup>139, 140</sup> In their first study, an alkoxyamine-functional poly(methylacrylate) initiator (PMA-SG1, where SG1 is *N-tert-butyl-N*-(1-diethylphosphono-2,2-dimethylpropyl) nitroxide) was employed to control <sup>n</sup>BuA polymerisation (up to 80% conversion), and high MW PSt and hexadecane were included to prevent Ostwald ripening. The emulsion was swollen overnight with St before reinitiation, and the resulting P<sup>n</sup>BuA-*b*-PSt had near quantitative blocking efficiency (measured by LAC analysis) and low  $\bar{D}$  (1.27). The authors noted that the reverse block copolymer (PSt-*b*-P<sup>n</sup>BuA) prepared by the same method had higher  $\bar{D}$  and lower blocking efficiency. The group later developed a more industrially-relevant *ab initio* emulsion NMP-controlled route to PSt-P<sup>n</sup>BuA block copolymers that shed light on some key reaction parameters affecting purity.<sup>122, 140</sup> *Ab initio* emulsion was compared to miniemulsion for the synthesis of P<sup>n</sup>BuA-*b*-PSt and ABA triblocks constituting P<sup>n</sup>BuA inner

block and either PSt or PMMA outer blocks (using a difunctional initiator).<sup>122</sup> The influence of <sup>n</sup>BuA conversion before St addition was evident in *ab initio* synthesis of P<sup>n</sup>BuA-b-PSt, with enhanced blocking efficiency and lower Đ being achieved when St was added at lower <sup>n</sup>BuA conversion (55% vs. 81%), but at the expense of block sequence purity. PSt-b-P<sup>n</sup>BuA-b-PSt prepared under *ab initio* conditions displayed lower block copolymer Đ than miniemulsion (1.64 vs. 3.95) and a high blocking efficiency (no detectable homo-P<sup>n</sup>BuA by LAC), although block sequence purity was lower. PMMA-b-P<sup>n</sup>BuA-b-PMMA prepared under *ab initio* conditions had a higher Đ than PSt-b-P<sup>n</sup>BuA-b-PSt (2 vs. 1.64) and a comparable high blocking efficiency (95%), even though SG1-controlled polymerisation of MMA alone is not usually well-controlled.<sup>141</sup> In contrast to the study by Bowes *et al.* that compared monofunctional and difunctional RAFT agents,<sup>106</sup> the difunctional alkoxyamine permitted an overall higher blocking efficiency than the monofunctional analogue (and comparable Đ). Furthermore, miniemulsion polymerisation permitted a more living process leading to higher blocking efficiencies than *ab initio*, although with very high Đ, which highlights that control within the different classes of emulsion polymerisation varies.

In an effort towards more industrially-viable aqueous NMP-controlled solvophobic block copolymer syntheses, Enright *et al.* conducted miniemulsion NMP in a continuous tubular reactor to synthesise PSt-b-P<sup>n</sup>BuA and PSt-b-P<sup>n</sup>BuA-b-PSt.<sup>123</sup> To accelerate polymerisation and ensure high conversion, ascorbic acid was added to consume free nitroxide. However, diblock and triblock Đ was high (~2), and there appeared to be significant dead homopolymer contamination. Blocking efficiency could be improved by decreasing the reaction time and monomer conversion at each step.

O'Connor *et al.* utilised scCO<sub>2</sub> as an alternative medium for a two-pot NMP-controlled synthesis of PDMA-b-PNIPAM, PAA-b-PNIPAM and PSt-b-PNIPAM.<sup>124</sup> Polymerisation of DMA, tert-butyl acrylate (<sup>t</sup>BuA) or St by SG-controlled precipitation NMP in scCO<sub>2</sub> led to polymers with Đ ranging from 1.13-1.23. After being purified by precipitation into hexane, chain extension with NIPAM was conducted in a suspension polymerisation in scCO<sub>2</sub>, which proceeded in a controlled manner. Block copolymer Đ (measured after purification) was lowest in P<sup>t</sup>BuA-b-PNIPAM and highest in PDMA-b-PNIPAM (from 1.3 to 2.1). Additional SG1 agent was a key component in the polymerisation, and served to counteract reagent partitioning into the continuous phase and loss of control. This study reaffirms the versatility of scCO<sub>2</sub> as a continuous phase solvent for solvophobic syntheses of a range of functional block copolymers.

## 2.d. Other CLRP

There have been a number of reports adopting the less common forms of CLRP for solvophobic block copolymer synthesis in water and  $scCO_2$ . Fuji *et al* synthesised  $P^nBuA$ - $b$ - $P^lBuA$ ,  $P^nBuA$ - $b$ - $PS$ t and  $P^lBuA$ - $b$ - $PS$ t in one pot processes using a half-metallocene iron(II)-catalyst, in which the mechanism is related to ATRP.<sup>125</sup> The surfactant-free suspension polymerisation in water enabled syntheses that would not have been possible under solution conditions without inclusion of specific additives. Blocking efficiency of the different copolymers could be qualitatively compared based on the appearance of low MW shoulder in GPC traces that arose from dead chains of the first block homopolymer. It appeared that  $P^nBuA$ - $b$ - $PS$ t had the highest blocking efficiency, and  $P^lBuA$ - $b$ - $PS$ t the lowest. Using  $P^lBuA$  as the first block necessitated a longer reaction time to achieve high conversion, during which more termination occurred leading to loss of livingness and lower blocking efficiency.

Tonnar *et al.* utilised reverse iodine transfer polymerisation (RITP) in an *ab initio* emulsion to synthesise  $P^nBuA$ - $b$ - $PS$ .<sup>126</sup> To counteract the hydrolytic degradation of  $I_2$  to HI in the aqueous phase, the highly oxidising initiator  $K_2S_2O_8$  was employed to regenerate iodine and initiate polymerisation simultaneously. Both  $nBuA$  and  $St$  polymerisations proceeded in a controlled manner and blocking efficiency was high based on GPC dual detection analysis, although the block copolymer possessed fairly high  $\bar{D}$  (1.8). This method demonstrated a simplification of the *ab initio* emulsion polymerisation process to one experimental step (relative to the many CLRP aqueous *ab initio* emulsion systems that involve intricate monomer feeding protocols) and without the use of a polymeric control agent **that becomes incorporated into the polymer and may alter the final properties.**

Kitayama *et al.* prepared  $PMMA$ - $b$ - $PBzMA$  by reversible chain transfer catalysed polymerisation (RTCP) in aqueous miniemulsion.<sup>87</sup> A miniemulsion of  $MMA$  was polymerised in the presence of  $N$ -iodosuccinimide before  $BzMA$  was added and allowed to swell the  $PMMA$  emulsion overnight before polymerisation. The resulting block copolymers had low  $\bar{D}$  (1.4) and high blocking efficiency (88%, measured by GPC dual detection). However,  $BzMA$  was added after 64%  $MMA$  conversion, which would result in significant block sequence impurity. This study importantly acknowledges the limitation of the GPC dual detection method in detecting newly initiated chains of second block homopolymer, which are indistinguishable from block copolymer if both are UV absorbing. These additional impurities

are seldom accounted for when calculating blocking efficiency by this method, but will be present in non-trivial quantities, particularly in processes where additional initiator is added with the second monomer and new chains are initiated. Kitayama *et al.* also carried out aqueous *ab initio* TERP for the synthesis of PMAA-*b*-P<sup>n</sup>BuA-*b*-PS.<sup>127</sup> Simultaneous emulsion stabilisation and polymerisation of <sup>n</sup>BuA was achieved *via* methyltellanyl functional poly(methacrylic acid) (PMAA-TeMe, the equivalent of a macro-RAFT agent). Although MW increased linearly with conversion, the resulting P<sup>n</sup>BuA had high Đ (~ 3). St was added with extra initiator, which resulted in a block copolymer with Đ = 1.8 and a blocking efficiency of 76% (by GPC dual detection). Control over block copolymer synthesis could be improved by increasing the St polymerisation temperature from 60 to 70 °C, which was attributed to a more homogeneous distribution of radicals between particles as a result of increased radical entry frequency. Although MW growth deviated from theory at both stages of polymerisation,<sup>89, 102-104</sup> the purity of the resulting polymers compared reasonably well to *ab initio* processes adopting macro-RAFT agents, implying that CLRP methods based on degenerative chain transfer mechanisms are equally applicable to solvophobic synthesis.

The Okubo group recently adopted scCO<sub>2</sub> as the medium for RTCP-controlled synthesis of PSt-*b*-PMMA, in a dispersion polymerisation stabilised and initiated using an azo-containing PDMS macroinitiator.<sup>128</sup> After controlled St polymerisation, MMA was added under pressure and the resulting block copolymer had high Đ (2.05), and a blocking efficiency of <75% (estimated by GPC dual detection). A particularly interesting aspect of this study is the observation that the RTCP mechanism was only effective in scCO<sub>2</sub>, proceeding in an uncontrolled/non-living manner in bulk, solution (toluene) and other heterogeneous systems (dispersion in hexane). This led to the conclusion that scCO<sub>2</sub> enhanced the reversible transfer step of the mechanism by plasticising polymer chains and facilitating the diffusion of GeI<sub>4</sub> catalyst, as previously argued by Howdle and coworkers for RAFT-controlled synthesis.<sup>120</sup> The synthesis of PSt-*b*-PMMA is normally problematic due the slow initiation of MMA by PSt macroradical, but becomes favourable in scCO<sub>2</sub>, which highlights an additional benefit of the medium as the continuous phase in solvophobic syntheses. ScCO<sub>2</sub> has also been exploited as a medium for cobalt-mediated radical polymerisation (CMRP) to synthesise poly(vinyl acetate)-block-poly(acrylonitrile) (PVAc-*b*-PAN) in a dispersion polymerisation.<sup>129</sup> Control over PVAc synthesis was maintained until 10 kg mol<sup>-1</sup>, above which precipitation occurred, and bimolecular termination led to an increase in dispersity. AN was added after removing unreacted VAc from the reactor by vacuum, and the scCO<sub>2</sub>-soluble PVAc block stabilised the

growing block copolymer particles. The resulting copolymers possessed high dispersity ( $\mathcal{D} = 2$ ) as a result of the low solubility of PAN in  $scCO_2$ .

## 2.e. Properties of block copolymers from solvophobic synthesis

The myriad industrially-friendly solvophobic syntheses inevitably lead to block copolymers with lower purity than from anionic polymerisations in terms of distribution of chain lengths (*i.e.*  $\mathcal{D}$ ), blocking efficiency, and purity of monomer sequences (Fig. 3). Ultimately, the significance of these impurities depends on their impact on final material properties and applications of the block copolymer. Since applications of block copolymers usually rely on their microphase separated structure, a number of the articles highlighted in Section 2a-2d also reported on the self-assembly and material properties of block copolymers synthesised within particles.

During solvophobic block copolymer syntheses, under the correct set of conditions, microphase separation may take place resulting in nanostructured particles comprising domains of the two blocks on the length scale of the polymer chains (typically 10 – 100 nm). In general, bulk block copolymer self-assembly into phase separated structures is governed by both the enthalpic interaction between the blocks, quantified by the Flory-Huggins interaction parameter  $\chi$ , and the total degree of polymerisation of the copolymer,  $N$ .<sup>142</sup> Usually, if the product of  $\chi$  and  $N$  exceeds 10.5, then block copolymers phase separate into domains whose morphology depends on the relative volume fractions of the two blocks (Fig. 6).<sup>143</sup> Depending on the proximity of the system to this critical number, the phase separation is described as strongly segregated ( $\chi N \gg 10.5$ ) or weakly segregated ( $\chi N \sim 10.5$ ).<sup>144</sup> Fundamental block copolymer self-assembly theory is founded on the notion that block copolymers consist of two pure, monodisperse sequences of monomers, but many variables are introduced when conducting solvophobic CLRP block copolymer synthesis in one pot. In particular, chain length dispersity,<sup>145, 146</sup> unreacted homopolymer from a process with low blocking efficiency,<sup>147, 148</sup> and mixed monomer sequences arising from the presence of unreacted monomer<sup>149</sup> can all profoundly affect block copolymer phase behaviour.

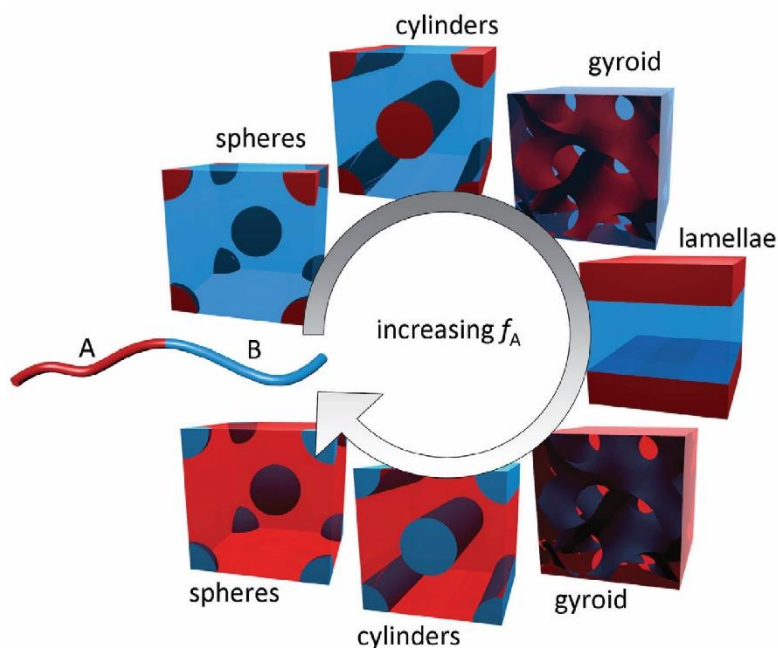


**Figure 6:** Schematic depicting the most commonly encountered morphologies resulting from self-assembly of diblock copolymers (AB), displayed in order of increasing block A volume fraction,  $f_A$ . Reproduced with permission from reference<sup>150</sup>, copyright Elsevier, 2010.

Unlike amphiphilic block copolymer synthesis (see Section 3), the mechanism of *in situ* self-assembly during solvophobic block copolymer synthesis has seldom been investigated nor discussed in the literature. Indeed, the onset of phase separation has been implicated with hindering chain transfer processes and leading to reduced control over polymerisation in solvophobic CLRP.<sup>107, 111</sup> Presumably, the mechanism involves growth of the second block until a critical condition is reached at which the two polymers become incompatible (i.e. “ $\chi N_{\text{crit}}$ ”) and phase separation takes place (Fig. 1). The exact value of  $\chi N_{\text{crit}}$  will be influenced by unreacted monomer, the continuous phase solvent, and surfactant/stabiliser, alongside the common factors associated with block copolymer self-assembly. In addition to block volume fraction, phase separated morphology can be influenced by confinement effects, typically when the ratio of particle size to polymer domain size is  $<2$ . Such confinement effects have been observed within particles prepared by controlled precipitation methods, and can lead to new and useful morphologies inaccessible in bulk block copolymer systems.<sup>151</sup>

This section of the review summarises reports where nanoscale morphology was investigated within particles from solvophobic synthesis, and/or where particles were reprocessed into microphase separated bulk materials or thin films, focussing on the influence



of polymer purity on the ultimate microphase separated structure. Furthermore, a few of these reports took block copolymer materials forward for property testing, which provides insight into the effect of impurities on potential future applications. For example, a number of studies target hard-soft triblock copolymers (*i.e.* PSt-b-P<sup>n</sup>BuA-b-PSt, PSt-b-PBd-b-PSt), which make effective thermoplastic elastomers (TPEs) when in the phase separated state.

### *i. ATRP*

The group of Okubo extensively studied phase separation of P<sup>i</sup>BuMA-b-PSt within submicron particles synthesised by miniemulsion ATRP.<sup>94-96</sup> In the initial study, the interior of near-symmetrical P<sup>i</sup>BuMA-b-PSt particles appeared onion-like, indicating phase separation into lamellar morphology, as expected based on volume fraction.<sup>94</sup> Results from the second study suggested an influence of blocking efficiency on phase separation. When blocking efficiency was ca. 40% (*i.e.* 60 mol% homopolymer), block copolymer particles had “sea-island” or disordered morphology, but when blocking efficiency was 61%, onion-like particles were observed. Notably, the disordered block copolymer also had lower MW and a higher  $\bar{D}$  than the phase separated system, which would further favour the disordered state. A later investigation revealed the influence of St polymerisation temperature on morphology.<sup>96</sup> At 70 and 90 °C, block copolymer particles with lamellar morphology resulted, but at the highest temperature (110 °C), the particles appeared disordered (Fig. 7). This trend was again attributed to the higher homopolymer impurity from the synthesis at 110 °C. The P<sup>i</sup>BuMA-PSt pair is thought to be a relatively weakly-segregated system (*i.e.* low  $\chi$ ),<sup>152</sup> which explains its tendency towards disorder when impurities are high.

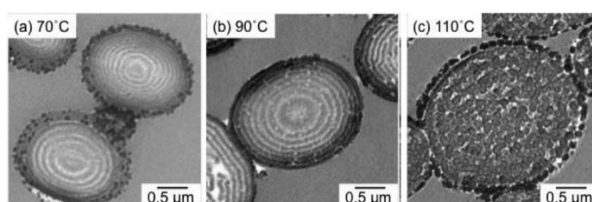


**Figure 7:** TEM images of nanostructured P<sup>i</sup>BuMA-b-PSt particles synthesised by ATRP in miniemulsion. The polymerisation temperature of St influenced the final morphology: from onion-like microphase separated structure at lower temperatures (A & B) to disordered

morphology at the highest temperature (C). Reproduced with permission from reference<sup>96</sup>, copyright ACS, 2010.

## ii. RAFT

Smulders and Monteiro were the first to observe block copolymer phase separation from a RAFT-controlled solvophobic synthesis, into core-shell nanoparticles of symmetrical PSt-b-(PBuA-co-PAAEMA),<sup>89</sup> despite homopolymer contamination (ca. 24%). The confinement to nanoparticles on the length scale of lamellar periodicity resulted in self-assembly into core-shell particles, rather than the multi-layer structures described above (Fig. 6). Preparing films from these particles by solvent casting and thermal annealing resulted in well-defined domains of PSt in a P<sup>n</sup>BuA matrix, however the migration of surfactant to the surface was noted to inhibit film homogeneity.<sup>102</sup> Sprone *et al.* later demonstrated means by which to influence the identity of core and shell blocks within symmetric PSt-b-P<sup>n</sup>BuA and PSt-b-(P<sup>n</sup>BuA-co-PMMA) particles.<sup>133</sup> Although the more hydrophobic PSt energetically prefers to form the particle core, using PAA-b-P<sup>n</sup>BuA-TTC produced core-shell particles with P<sup>n</sup>BuA cores. Alternatively, using PAA-b-PSt-TTC resulted in unusual deformed particles with mixed shells comprising inclusions of PSt amongst domains of the more hydrophilic P<sup>n</sup>BuA-co-PMMA. A simple method to control the thickness of the shell in P<sup>n</sup>BuA-b-PSt particles by modifying the length of the P<sup>n</sup>BuA block was reported by Yang *et al.*<sup>111</sup> High <sup>n</sup>BuA conversion ensured pure block sequences, and phase separation was observed at a range of MWs. The functionality of the reactive macro-RAFT agent (containing PGIMA) assisted coalescence when preparing block copolymer films, which developed a morphology of spherical PSt nano-domains in a P<sup>n</sup>BuA matrix. Notably, the use of an amphiphilic macro-RAFT that is covalently attached to the block copolymer should alleviate issues relating to small molecule surfactant migration to the film surface. However, the covalent attachment of a hydrophilic block will undoubtedly influence some bulk properties of the block copolymer, a factor that is yet to be investigated.

The influence of block sequence purity on microphase separation was uncovered by Guo *et al.*<sup>109</sup> through the deliberate synthesis of well-defined gradient copolymers in *ab initio* emulsion (PSt-grad-P<sup>n</sup>BuA, PSt-grad-P<sup>n</sup>BuA-grad-PSt and PSt-grad-PMA) and study into the phase separated structures in solvent cast films. PSt-grad-P<sup>n</sup>BuA and PSt-grad-P<sup>n</sup>BuA-grad-PSt copolymers with a continuous monomer gradient revealed poorly-defined microphase separation relative to their block copolymer analogues (Fig. 8). However,

the more strongly segregating PSt-grad-PMA formed a coarse phase separated structure, more comparable to PSt-b-P<sup>n</sup>BuA block copolymer at the same molecular weight. These findings suggest that block copolymers with very low block sequence purity can still form well-defined phase separated structures, if the polymer pair has sufficiently high  $\chi$ .

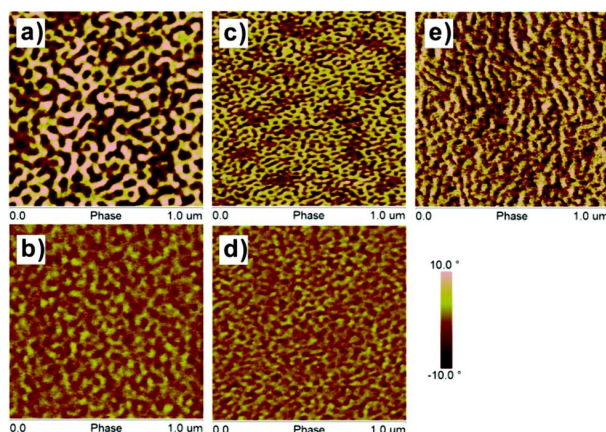


**Figure 8:** AFM images of films prepared from block (A, C) and gradient (B, D, E) copolymers synthesised by *ab initio* RAFT polymerisation. Phase separated structures from PSt-b-P<sup>n</sup>BuA (A) and PSt-b-P<sup>n</sup>BuA-b-PSt (C) were more well-defined than PSt-grad-P<sup>n</sup>BuA (B) and PSt-grad-P<sup>n</sup>BuA-grad-PSt (D). However, phase separation in PSt-grad-PMA (E), a more strongly segregating polymer pair, was comparable to PSt-b-P<sup>n</sup>BuA block copolymers. Adapted with permission from reference<sup>109</sup>, copyright RSC, 2014.

With a view to fabricating TPEs from a solvophobic synthesis, Luo *et al.* synthesised SBAS nanoparticles by *ab initio* RAFT polymerisation, acknowledging that any unreacted diblock copolymer or homopolymer would be degrading to mechanical properties.<sup>107</sup> Whilst morphology within the symmetrical copolymer particles was non-descript, upon casting films from THF reasonably well-defined lamellar morphology was evident, suggesting that a confinement effect drove the non-descript structure within particles. Dynamic mechanical analysis was employed to elucidate properties of the triblock copolymers relevant to TPEs. Measured values for tensile strength and elongation at break were almost comparable to benchmark TPEs synthesised by anionic polymerisation.<sup>135</sup> This finding implies that lower purity block copolymers from heterogeneous CLRP syntheses may still be able to compete with industry standard mechanical materials. This idea was reinforced by Zhan *et al.*, who synthesised SBAS by RAFT miniemulsion, which also performed comparably to conventional TPEs despite their high  $\bar{D}$  (3) and poorly ordered “sea-island” nanostructure.<sup>110</sup>

The development of microphase separated morphology within PSt-b-PBd nanoparticles during the Bd polymerisation step of a miniemulsion RAFT polymerisation was studied by Wei *et al.*<sup>113</sup> With increasing PBd volume fraction, the morphology changed from spherical domains of PBd in a PSt matrix to lamellar, then bicontinuous, before concluding with domains of PSt in a PBd matrix. The final morphology was thought to be kinetically trapped as a result of either PBd cross-linking during polymerisation or spherical confinement. The authors acknowledged that block sequence purity was low owing to the incomplete conversion of St in the first step (81%), but due to the strongly segregating nature of the polymer pair, microphase separation was observed as early as 5% Bd conversion. At each stage, different morphologies were observed inside particles of different sizes, alluding to an effect of confinement on block copolymer self-assembly. The group also studied near-symmetrical PBd-b-PSt particles, in which cross-linking was avoided by reversing the block order.<sup>114</sup> The resulting particles appeared non-spherical and somewhat patchy, similar to those observed by Hawke<sup>133</sup> which suggested that the particle distorted from the expected core-shell structure to minimise the area of contact between PBd and water. A recent publication by Froimowicz *et al.* shed light on PSt-PBd microphase separation within larger particles from solvophobic synthesis that far exceeded the length scale of the polymer chains.<sup>116</sup> Core-shell particles of PBd-b-PSt-b-PBd with very high blocking efficiency but low block purity comprised bilayer shells at ~60% PBd, and microphase separated lamellar-patterned shells at ~90% PBd. However, the particle interior appeared unstructured in all cases, which may be a result of the low block sequence purity leading to miscibility between PSt and PBd. Films have also been prepared from PSt-PBd copolymers synthesised by solvophobic syntheses, initially by Wei *et al.*, who utilised PSt-b-PBd-b-PSt triblock copolymer (SBS) synthesised by miniemulsion RAFT as TPEs.<sup>115</sup> Films cast from solutions in THF evaporated over 3 days displayed fairly well-defined worm-like and partial lamellar morphologies as the volume fraction of PSt was increased. Despite high  $\bar{D}$ , the ultimate tensile strengths exceeded those found by Luo *et al.* for PSt-b-P<sup>n</sup>BuA-b-PSt synthesised by miniemulsion RAFT,<sup>107</sup> and approached values associated with SBS synthesised in anionic solution polymerisation.<sup>135</sup> Films of PSt-b-(PSt-co-PBd) (i.e. with low PBd block sequence purity) prepared by Wang *et al.* revealed well-defined lamellar and cylindrical structures when MW was sufficiently high ( $>25 \text{ kg mol}^{-1}$ ),<sup>137</sup> coinciding with calculated values of  $\chi N > 10.5$ .

Self-assembly within block copolymer particles synthesised by RAFT  $\text{scCO}_2$  dispersion was studied by Jennings *et al.*<sup>119</sup> Phase separated structures were observed in a

variety of copolymers, despite some relatively low blocking efficiencies (>50%) and high dispersity ( $\bar{D} = 2$ ).<sup>120</sup> Particles of symmetrical PMMA-*b*-PBzMA and PMMA-*b*-PDMAEMA revealed lamellar phase separated morphology, whilst symmetrical PMMA-*b*-PSt and PMMA-*b*-P4VP showed cylinders and spheres, respectively (Fig. 9). The authors proposed that final self-assembled morphology depended on relative CO<sub>2</sub>-philicity of the two blocks, leading to a selective solvent effect. In a follow up study the influence of scCO<sub>2</sub> was further **proven by preparing block copolymer films cast from solutions**, in which morphologies had returned to equilibrium structures predicted by volume fraction. Furthermore, the selective solvent effect of CO<sub>2</sub> was exploited as a means to change phase separated morphology by simply changing initial monomer concentration, and subsequently the polymer:CO<sub>2</sub> ratio, during synthesis.<sup>138</sup> The authors developed a high pressure SAXS cell in order to monitor the progression of morphology during polymerisations, and experiments to provide insight into the mechanism of self-assembly during solvophobic block copolymer synthesis are underway.<sup>153</sup> Studies into phase behaviour of block copolymer particles dispersed in scCO<sub>2</sub> demonstrates that the continuous phase solvent in a solvophobic synthesis can influence block copolymer phase separation, if the relative solubility in one of the polymer blocks is adequate.

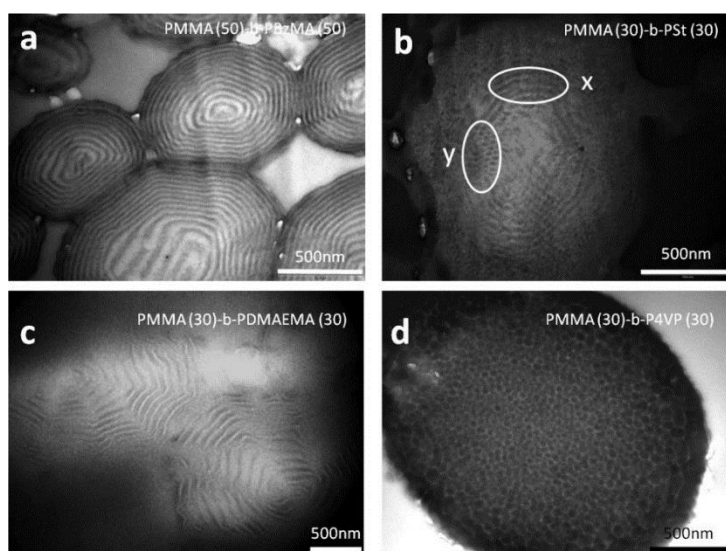


**Figure 9:** TEM images demonstrating different morphologies observed within microparticles of near-symmetrical block copolymers synthesised by RAFT scCO<sub>2</sub> dispersion. (a) PMMA-*b*-

PBzMA: lamellar; (b) PMMA-b-PSt: cylindrical (the regions labelled x and y demonstrate views perpendicular to and along the cylinder axis, respectively); (c) PMMA-b-PDMAEMA: lamellar; and (d) PMMA-b-P4VP: spherical. The numbers in brackets denote the theoretical molecular weight of each block, determined by the molar ratio of monomer to RAFT agent used in the synthesis. Reproduced with permission from reference <sup>119</sup>, copyright ACS, 2012.

### iii. NMP

The most thorough report of block copolymer microphase separation from a solvophobic NMP synthesis originated from Nicolas *et al.*, who prepared submicron particles of P<sup>n</sup>BuA-b-PS, PSt-b-P<sup>n</sup>BuA-b-PS, and PMMA-b-P<sup>n</sup>BuA-b-PMMA by miniemulsion or *ab initio* NMP.<sup>122</sup> This study effectively highlighted the impact of the three different block copolymer impurities (Fig. 3) on self-assembly within particles. From *ab initio* synthesis, particles of near symmetrical P<sup>n</sup>BuA-b-PSt and PMMA-b-P<sup>n</sup>BuA-b-PMMA microphase separated with lamellar morphology (e.g. Fig. 10A). Despite the exceptionally high  $\Phi$  (4) of PSt-b-P<sup>n</sup>BuA-b-PSt synthesised in miniemulsion, the particles also revealed a well-defined lamellar nanostructure (Fig. 10B). However, when St was added for <sup>n</sup>BuA conversion below 80%, the resulting copolymers were disordered, even after thermal annealing (Fig. 10C). The authors quantified the effect of block sequence purity on miscibility by calculating the decrease in effective  $\chi$  between a pure P<sup>n</sup>BuA block and a P<sup>n</sup>BuA-co-PSt block. The P<sup>n</sup>BuA-PSt pair is considered a moderately segregating system,<sup>152</sup> and this study implies that block sequence purity is the dominating factor driving phase separation in this system.

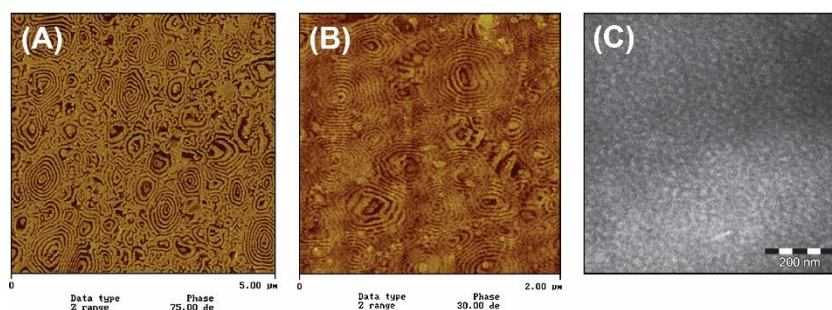


**Figure 10:** AFM (A-B) and TEM (C) images of block copolymers synthesised by *ab initio* emulsion (A and C) or miniemulsion (B) NMP. PMMA-b-P<sup>n</sup>BuA-b-PMMA (A) and PSt-b-P<sup>n</sup>BuA-b-PSt (B) particles were dried at room temperature before imaging. P<sup>n</sup>BuA-b-PSt (C)

particles were dried at room temperature, annealed at 150 °C and stained prior to imaging. The lower block sequence purity of the copolymer in C led to a smaller  $\chi$  and the formation of a disordered morphology. Adapted with permission from reference<sup>122</sup>, copyright Elsevier, 2007.

## 2.f. Solvophobic Block Copolymer Synthesis: Discussion

An increasing number of studies into solvophobic block copolymer syntheses by CLRP are emerging, driven by the desire to apply industrially relevant conditions to the synthesis of block copolymer materials with advantageous properties. Numerous methods of CLRP have been applied to heterogeneous polymerisation, primarily using water or scCO<sub>2</sub> as the continuous phase. The ability to conduct syntheses under benign conditions, *i.e.* atmospheric pressure, low temperature and with green solvents and reagents, is a priority when considering industrial application. Thus, NMP-controlled polymerisations are less coveted due to the usual requirement for higher temperatures. Furthermore, CLRP processes that are less sensitive to atmospheric oxygen are sought, for example AGET ATRP is more commonly employed than conventional ATRP.

Of all the heterogeneous polymerisation processes, *ab initio* emulsion is the most attractive, considering its current application in numerous industrial latex syntheses.<sup>1</sup> Although the process is relatively simple, the complexity of the mechanism often impedes compatibility with CLRP techniques, necessitating the development of new protocols that move away from a one-pot approach or add further processing or synthetic steps that are potentially unfavourable from an industrial standpoint. Arguably the most promising modification of *ab initio* CLRP is the use of a macroCTA or macroinitiator that also functions as a surfactant, which typically enables simultaneous control over the polymerisation and colloidal stability, and as such the strategy is now commonplace.<sup>133, 107, 108, 109, 111, 114, 112, 117</sup> In RAFT, using an amphiphilic macro-RAFT agent immediately localises the CTA at the polymerisation loci, *i.e.* within micelles. However, use of polymeric CTAs or initiators still adds a synthetic step to the procedure, and the covalent attachment of the additional block could significantly modify the desired properties of the resulting copolymer. Some simple and effective process modifications to *ab initio* for enhancing block copolymer purity (*i.e.* increasing blocking efficiency and decreasing  $\bar{D}$ ) include allowing the first polymer block to swell with second monomer prior to reinitiation, and controlling the feed rate of the second monomer.

Miniemulsion polymerisation provides a simplified reaction environment in which to conduct CLRP, but is often dismissed industrially due to the need for high energy input to create the kinetically stable miniemulsion, and the resulting particles often possess a broader particle size distribution relative to emulsion polymerisation.<sup>3</sup> Furthermore, a critical comparison of studies listed in Table 1 indicates that on average polymerisation control is poorer in miniemulsion (i.e. higher  $\bar{D}$ ) than *ab initio*, although absolute comparison of blocking efficiency in different studies is difficult. The potential of microemulsion polymerisation has yet to be fully realised for solvophobic block copolymer syntheses, although the few published examples suggests that highly pure products can be obtained,<sup>97, 118</sup> which may be a direct result of confinement effects, where termination and radical side reactions are suppressed.<sup>154, 155</sup>

Methods in which the monomer is initially soluble and the growing polymer precipitates can further simplify the polymerisation process *i.e.* dispersion and precipitation polymerisation. There are examples of aqueous dispersion polymerisation,<sup>156-158</sup> but monomers applicable to this technique are rare.  $\text{ScCO}_2$  provides a more universal solvent for dispersion polymerisation, since it dissolves most monomers, but all polymers with the exception of highly fluorinated polymers,<sup>159</sup> siloxane-based polymers<sup>160</sup> and a small subset of hydrocarbon polymers,<sup>161-163</sup> are insoluble. Consequently, this solvent has been applied heterogeneous CLRP synthesis of block copolymers with a wide range of chemical functionality and should provide access to a range of block copolymers not accessible by a solvophobic route in other solvents (e.g. hydrophilic-hydrophobic block copolymer particles). However, the requirement for specialist equipment (reactors, high pressure pumps, etc.) has up until now restricted the development of this technique in a large-scale industrial setting.<sup>164</sup> An ideal solvophobic synthesis would forego the need for surfactant/stabiliser altogether (*i.e.* precipitation polymerisation), since these additional components are difficult to separate and could be degrading to bulk or surface properties of the polymer. However, there are relatively few examples of successful CLRP block copolymer syntheses in precipitation polymerisations,<sup>101, 121, 124</sup> probably due to challenges in controlling reagent partitioning and particle aggregation.

When selecting a method of CLRP for solvophobic synthesis with an application in mind, one must consider the control agent, which imposes specific polymerisation conditions, restricts the range of monomers that can be polymerised in a controlled manner, and often dictates the order of block synthesis (although some have showed that colloidal stability must also be considered when selecting the block order<sup>106</sup>). However, it has also been demonstrated in the Monteiro group<sup>102, 103</sup> that polymerisation of more activated monomers can be controlled



using xanthates (which are notably commercial<sup>165</sup>), from which it can be concluded that reactivity matching of RAFT agent with monomer is not a prerequisite for solvophobic synthesis of block copolymers. The CLRP technique should be robust, in that all reagents used should have minimal sensitivity to oxygen and optimal solubility within the system (particularly for copper catalysts). These challenges are arguably best matched by a RAFT-controlled approach, which may explain why RAFT solvophobic polymerisations are the most numerous, and lead to block copolymers with higher purity on average. Results of RAFT-controlled studies strongly suggest that the intrinsic kinetic parameters for a given monomer system (*i.e.*  $k_p$ ,  $k_t$ ) influence the maximum achievable blocking efficiency, and the more rapidly polymerising *high*  $k_p$  monomers (e.g. acrylates, acrylamides) that enable shorter polymerisation times are the optimal choice for the first block. Of the studies reviewed above, solvophobic block copolymer syntheses adopting P<sup>n</sup>BuA as the first block typically achieve the highest blocking efficiencies coupled with high monomer sequence purity, which may be an intrinsic feature of all monomers with these characteristics. It is important to note that within degenerative chain transfer processes, the initial concentration of radical initiator relative to the control agent governs the proportion of dead chains. Therefore, by controlling the conditions, extremely high livingness and block copolymer purity can be achieved, a concept that was recently explored by Gody *et al* in a homogeneous system.<sup>31, 36 35 33, 166, 167</sup> Within these studies monomers with high rate of propagation (*i.e.* acrylates and acrylamides) were exploited to rapidly synthesise multiblock copolymers without purification steps, and in one pot, an enticing prospect for future work in solvophobic synthesis.

Ultimately, it is the ability of block copolymers to microphase separate that dictates the success of the synthetic procedure. Block copolymers from solvophobic syntheses can be considered to contain substantial impurities (Fig. 3): often having very high  $\bar{D}$  (up to 4), low blocking efficiency (up to 50% homopolymer contamination), and when the synthesis is conducted in one pot, low block sequence purity. In general, livingness and hence blocking efficiency can be maximised by stopping a reaction at lower conversion, but in a one-pot environment the unreacted monomer leads to significant block sequence impurity. Both homopolymer contamination<sup>96</sup> and block sequence impurities<sup>122</sup> can lead to degradation of a phase separated structure and may affect resulting material properties. Based on the reviewed literature above, we can provide guidelines on how to compromise between these two competing factors and obtain microphase separated block copolymer materials from a solvophobic synthesis. In most block copolymer pairs studied, the block sequence impurity

imparted by chain extension after a first monomer conversion of 80% does not preclude a phase separated state, provided the molecular weight is sufficiently high. This conversion can realistically be achieved with minimal loss of livingness and fewer side reactions, ensuring blocking efficiency remains high and the molecular weight distribution near monodisperse. By careful selection of monomer pairs which impart the desired block copolymer properties, materials can be tailored to specific applications. For example, the solvophobic synthesis of TPEs based on SBAS (PSt-*b*-P<sup>n</sup>BuA-*b*-PSt) has proven to be more well-controlled than solvophobic synthesis of SBS (PSt-*b*-PBd-*b*-PSt) (due to cross-linking in the latter), and it has been demonstrated that material properties can be achieved that are comparable to the current benchmark TPE materials.<sup>107, 110, 115</sup>

### 3. Amphiphilic Block Copolymers by CLRP in Dispersed Systems

While the previous section summarised CLRP block copolymer synthesis where two or more blocks are insoluble in the continuous phase, this section deals with syntheses in which polymerisation of **only the final** block takes place in a dispersed phase, and **the initial** block or blocks are soluble in the continuous phase. The first step is usually the synthesis of a soluble macroCTA or macroinitiator (either *in situ* or in a separate step) **followed by chain extension with a new soluble or insoluble monomer** to generate an amphiphilic block copolymer able to undergo self-assembly into particles. This process typically adopts one of the established CLRP techniques in connection with particle formation *via* self-assembly of the amphiphilic block copolymer formed *in situ*, in a similar manner to the first step of the modified *ab initio* emulsion techniques described in Section 2. This phenomenon is often termed “Polymerisation Induced Self-Assembly” (PISA), and affords polymeric nano-objects such as **spheres**, worms/fibres/rods/cylinders and vesicles (Fig. 2). Such approaches can be implemented either as an *ab initio* emulsion polymerisation<sup>168-172</sup> or as a dispersion polymerisation,<sup>157, 173-178</sup> in which the continuous phase is typically water, or an alcohol/water mixture, respectively.

During the first years following the seminal paper by Gilbert, Hawket, and coworkers,<sup>168</sup> all reports on emulsion polymerisation involving *in situ* formed amphiphilic block copolymers yielded spherical nano-objects. Later, it was realised that under suitable experimental conditions, a wider range of morphologies such as worms and vesicles can also be accessed *via* this technique. The final morphology can be rationalised by the packing parameter,  $P = v/al$  which was first introduced by Israelachvili for small molecule surfactants.<sup>179</sup> For an amphiphilic diblock copolymer,  $v$  and  $l$  are the volume and the length of the hydrophobic block, respectively, and  $a$  is the effective interfacial area of the block junction. However, calculation of  $P$  for block copolymers is non-trivial and the *in situ* polymerisation adds extra complications, such as unreacted monomer and partial solvation of the core-block.<sup>178, 180</sup> Experimental phase diagrams provide an opportunity to target specific morphologies in amphiphilic block copolymers, however, more specific theoretical studies are desirable in this area.

In addition to the updated review published by Zetterlund *et al* on CLRP in dispersed systems,<sup>181</sup> there have been several excellent reviews outlining PISA of amphiphilic block copolymers synthesised by CLRP, most of which are specific to RAFT-controlled systems.<sup>182-186</sup> In the following sections (3a-3e), we summarise the different CLRP methods, numerous monomers and variety of solvents used in emulsion- and dispersion syntheses of amphiphilic block copolymers, while simultaneously discussing the nano-objects formed by PISA.

### 3.a. ATRP in emulsion/dispersion

In reports of ATRP-controlled synthesis of amphiphilic block copolymers, a two-step approach is typically adopted, in which a macro-initiator such as PEG-X (X=Br or Cl) is pre-synthesised before addition of the hydrophobic monomer. As discussed earlier, a problem specific to ATRP systems is partitioning of the catalyst, usually a transition metal complex, which can have a detrimental effect on the control of polymerisation. One approach to avoid the Cu(II) partitioning to the aqueous phase is to use seeded emulsion polymerization by encapsulating the Cu catalyst in a preformed microlatex which is used as the seed for emulsion polymerisation.<sup>92, 187</sup> AGET ATRP, in which a Cu(II) species is used and reduced to Cu(I) *in situ* by e.g. ascorbic acid, is particularly applicable in miniemulsion systems, and careful selection of a highly hydrophobic ligand for Cu curtails partitioning to the aqueous phase.<sup>73</sup>

There are relatively few examples of ATRP-controlled synthesis of amphiphilic block copolymers in emulsion or dispersion, and the resulting PISA. Kim *et al.* first reported the preparation of PEG-*b*-PNIPAM nanoparticles by ATRP in aqueous dispersion polymerisation, exploiting the lower critical solution temperature (LCST) property of PNIPAM.<sup>188</sup> From a PEG-Br macro-initiator, NIPAM was polymerised at either 25 or 50 °C. At 50 °C (above the LCST of PNIPAM), the block copolymer phase separated into micelles during NIPAM polymerisation, and the reaction took place as a dispersion. A number of notable examples originate from the Armes group, in particular the synthesis of zwitterionic poly(2-(methacryloyloxy)ethyl phosphorylcholine) (PMPC)-based block copolymers by dispersion ATRP.<sup>189, 190</sup> In the first study, PEG-Br was used as macro-initiator with CuBr/bpy as the catalyst for dispersion polymerisation of PMPC in isopropanol/water (9:1, w/w). The block copolymers had low dispersity ( $\mathcal{D} = \sim 1.2$ ), block composition agreed very well with the target, and polymerisation was rapid (complete in 8h). By using ethylene glycol dimethacrylate (EGDMA) as cross-linker hydrogel particles were obtained, and particle size could be controlled by the target block composition and initial MPC concentration. Using a similar strategy, the group synthesised well-defined PEG-*b*-PDMAEMA-*b*-PMPC triblock copolymer in one-pot ( $\mathcal{D} = 1.2$ ),<sup>190</sup> and nanocages with cross-linked shells could be obtained by subsequent cross-linking of the PDMAEMA chains in the same reaction solution.

### 3.b. RAFT Dispersion Polymerisation

The first attempts at RAFT dispersion polymerisation to yield amphiphilic block copolymers were reported around 2006, in which cyclohexane,<sup>173</sup> chloroform<sup>191</sup> and methanol<sup>174, 192-194</sup> were used as the continuous phase to prepare core-shell spheres. Pan *et al.*<sup>173</sup> first reported the polymerisation of 4VP in cyclohexane using PSt-DTB as macro-RAFT. Both plots of monomer conversion and copolymer MW against time showed a turning point at  $\sim 5$  h, which indicated micelle formation when the chain length of P4VP increased to a critical value. Block copolymers with unimodal GPC traces and low  $\mathcal{D}$  ( $< 1.1$ ) were achieved. A small quantity of divinylbenzene (DVB) was copolymerised with 4VP in order to obtain cross-linked micelles whilst avoiding macroscopic gelation. Kinetic studies demonstrated a sudden decrease of polymerisation rate and sharp increase of MW after 32% conversion, which was attributed to the restriction of diffusion and a higher concentration of macro-RAFT in the **micelle cores**. **Pan's group** also reversed the block order and carried out the polymerisation of St in methanol with a P4VP-TTC macro-RAFT,<sup>174, 175, 195, 196</sup> achieving non-spherical nano-objects (rods and

vesicles) by tuning the molar feed ratios of St/P4VP-TTC/AIBN/CH<sub>3</sub>OH (Fig. 11).<sup>174, 175</sup> When more St was added to the dispersion system to swell the PSt cores, the rate of polymerisation was maintained after morphological transition. The low dispersity ( $\mathcal{D} < 1.25$ ) of the resultant block copolymers and uniform assemblies demonstrate excellent control of polymerisation in this RAFT dispersion system, and the critical compositions required to form either rod-like micelles or vesicles were determined to be P4VP<sub>99</sub>-*b*-PS<sub>770</sub> and P4VP<sub>99</sub>-*b*-PS<sub>2040</sub>, respectively (Fig. 11D, top and 11F, bottom).

The macro-RAFT agents PEG-TTC,<sup>197</sup> PDMAEMA-DTB<sup>192</sup> and PAA-TTC<sup>193</sup> were also utilised to control dispersion polymerisation of St in methanol. By varying the feed ratio of St/CH<sub>3</sub>OH, St/macro-RAFT and/or macro-RAFT/AIBN, different morphologies were obtained. At a fixed feed ratio of St/CH<sub>3</sub>OH, it was found that increasing the ratio of St/macro-RAFT led to more complex assemblies, including concave spheres and kippah vesicles.<sup>193</sup> Perrier and coworkers<sup>198</sup> employed cryo-TEM to demonstrate that the morphologies observed after St polymerisation using PEG-methyl ether acrylate or methacrylate (P(PEG<sub>454</sub>A) and P(PEG<sub>475</sub>MA), respectively) in water/dioxane at 44 °C were indeed obtained during the polymerisation process itself, as opposed to being driven by selective solvent or solvent evaporation during TEM preparation.

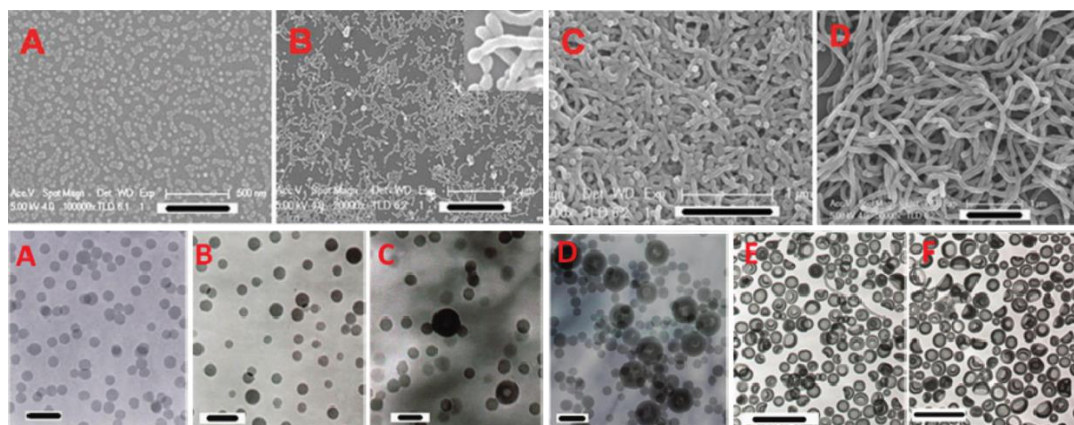


**Figure 11:** Morphology development during RAFT dispersion polymerisation of St in methanol with P4VP-TTC as macro-RAFT agent, showing morphologies obtained under various ranges of feed ratios and conditions. Top (A-D) feed molar ratio of P4VP/St/AIBN = 10 : 5 x 10<sup>4</sup> : 1 and 1 g St in 0.7 g methanol. (A) 3 h, (B) 4 h, (C) 12 h, (D) 24 h. Bottom (A-F) feed molar ratio of P4VP/St/AIBN = 10 : 1 x 10<sup>5</sup> : 1 and 2 g St in 1 g methanol. (A) 2 h, (C) 4 h, (D) 6 h, (E) 12 h, (F) 24 h. Scale bars: top (A) 500 nm, (B) 2000 nm, (C and D) 1000 nm;

bottom (A) 100 nm, (B, C and D) 200 nm, (E and F) 1000 nm. Adapted with permission from Ref. <sup>81</sup>, copyright RSC, 2009, and Ref. <sup>175</sup>, copyright ACS, 2009.

Zetterlund and coworkers<sup>199</sup> conducted PISA of St using a P4VP macro-RAFT agent in isopropanol and ethanol/water, expanded with low pressure (6.5-8 MPa) CO<sub>2</sub>. Both with and without CO<sub>2</sub>, MW increased almost linearly with conversion and Đ was relatively low (<1.4), although MW in the presence of CO<sub>2</sub> was significantly lower than theoretical MW for reasons that remain to be clarified. Importantly, the morphology could be tuned continuously *via* CO<sub>2</sub> without altering the polymerisation recipe. The presence of CO<sub>2</sub> delayed the morphological transitions from spheres to rods and to vesicles, and a wider window of each morphology was achieved in CO<sub>2</sub>. This could be due to the increased partitioning of St to the continuous phase, the increased solubility of PSt block in the presence of CO<sub>2</sub> and/or the volumetric expansion of PSt with CO<sub>2</sub>. Very recently, PEG (200 to 1000 Da) was used as a medium to synthesise a range of diblock copolymers via RAFT dispersion polymerisation.<sup>200</sup> Rapid polymerisation (>95 % conversion within 24 h) was achieved for St using various macro-RAFT agents, including PEG-TTC, PDEGMA-TTC, PDMA-TTC, P4VP-TTC, and PNIPAM-TTC. The viscous PEG medium enhanced polymerisation rate and led to unusual morphologies (ellipsoidal vesicles and nanotubes) up to a high solids content of 50 %. As another alternative to volatile organic compounds (VOCs), Zhang's group exploited an ionic liquid as the medium for RAFT dispersion polymerisation.<sup>201</sup> PEG-TTC mediated polymerisations of St in ionic liquid were faster than those in alcoholic solvent and afforded good control over MW and MW distribution (Đ<1.22).

Aqueous dispersion systems require that the monomer is water-soluble and the corresponding homopolymer is water-insoluble under reaction conditions, criteria which only a limited number of vinyl monomers fulfil, including NIPAM, DEAA, 2-methoxyethyl acrylate (MEA), 2-hydroxypropyl methacrylate (HPMA), and di(ethylene glycol) methyl ether methacrylate (DEGMA).<sup>182</sup> The Armes group have pioneered aqueous RAFT dispersion polymerisation for the synthesis of nonspherical nano-objects. In particular, macro-RAFT agents based on either poly(glycerol monomethacrylate) (PGMA),<sup>177</sup> PMPC,<sup>157</sup> or PEG<sup>178</sup> have been developed and chain extended with HPMA to yield worms or vesicles. The first phase diagram for such a PISA process focused on a PMPC<sub>25</sub> macro-RAFT with PHPMA as core-block.<sup>157</sup> It was found that the particle morphology obtained at full monomer conversion was dictated by the target degree of polymerisation (DP) of the hydrophobic PHPMA block and the total solids content. At low total solids content (10 w/w%), only spheres were obtained, even

at a high DP of the PHPMA block (400). When the total solids content was increased (25 w/w%), both rods and vesicles were produced as the DP of PHPMA block increased from 275 to 400. Further careful monitoring of the polymerisation by TEM analysis gave important mechanistic insights regarding the evolution of the particle morphology,<sup>176</sup> and spheres were observed fusing into dimers and further into linear worms. As polymerisation proceeded further, branched worms developed into nascent bilayers that eventually formed “jellyfish tentacles” before enclosing to form vesicles (Fig. 12). Later, a detailed phase diagram was reported from macro-RAFT agents PGMA<sub>78</sub>-DTB and PGMA<sub>47</sub>-DTB and variable lengths of PHPMA.<sup>177</sup> For the PGMA<sub>78</sub>-DTB, only spheres were obtained at low solid content of 10 w/w%, even at very high DP of PHPMA block of 500. Using the shorter PGMA<sub>47</sub>-DTB, a full range of morphologies including spheres, worms, and vesicles were obtained depending on the DP of PHPMA block at solids content between 10 – 25 w/w% (Fig. 13). These data appeared to indicate that the longer stabiliser blocks have sufficiently high steric stabilisation to hinder spherical micelle fusion at the time scale of HPMA polymerisation. In a recent study, the group investigated the sphere growth mechanism during RAFT dispersion polymerisation of BzMA using PDMAEMA-TTC as macro-RAFT,<sup>202</sup> which was ascribed to both the increase of copolymer MW and exchange of copolymer chains between micelles and/or the fusion of spheres.

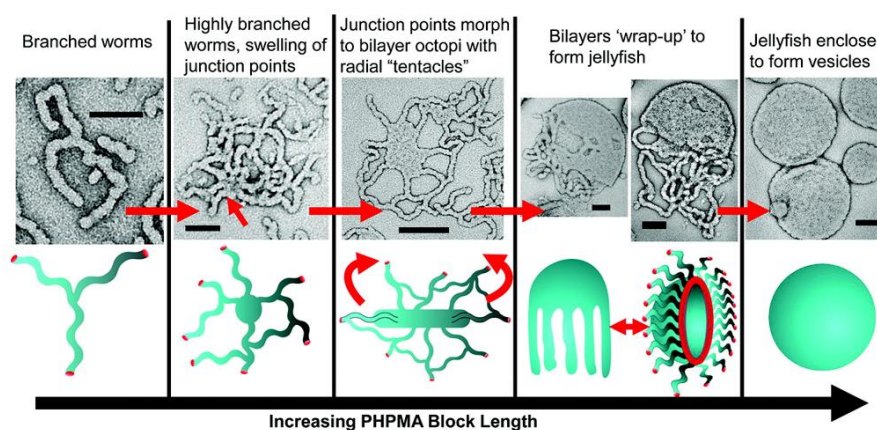


**Figure 12:** Intermediate morphologies observed during the polymerisation-induced worm-to-vesicle transformation in the synthesis of PGMA-*b*-PHPMA by aqueous RAFT dispersion polymerisation using PGMA as macro-RAFT. Reprinted with permission from Ref. <sup>176</sup>, copyright ACS, 2011.

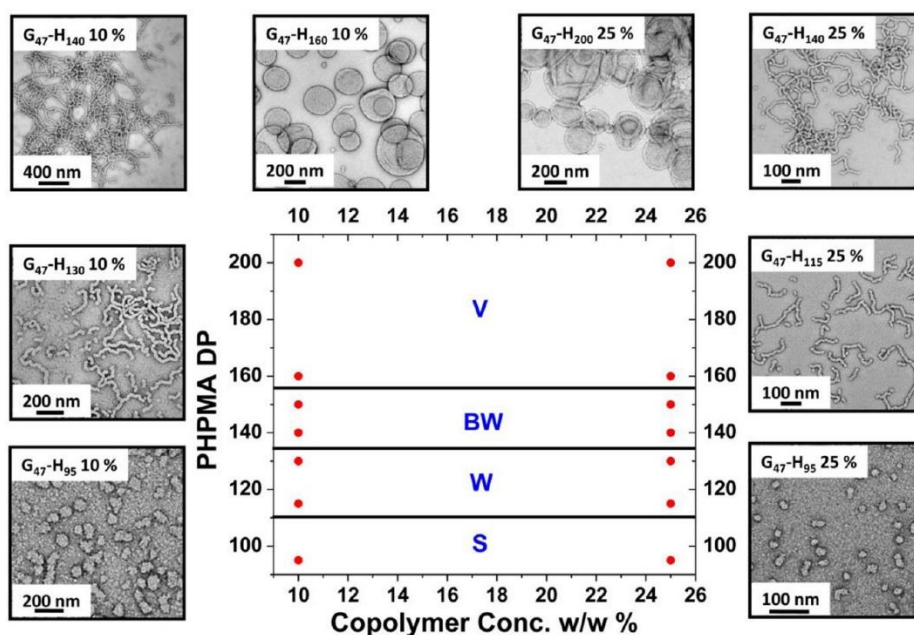


**Figure 13:** Phase diagram and the corresponding TEM images for aqueous RAFT dispersion polymerisation of PGMA-*b*-PHPMA ( $G_x$ - $H_y$ ) S = spherical micelles, W = worms, BW = branched worms, and V = vesicles. Reprinted with permission from Ref. <sup>177</sup>, copyright ACS, 2012.

Triblock copolymer nano-objects were recently prepared in the group of Zhang by chain extending the bifunctional macro-RAFT agents TTC-PNIPAM-TTC and TTC-P4VP-TTC (pre-synthesised) with St *via* dispersion polymerisation.<sup>203, 204</sup> St polymerisation from the bifunctional RAFT was slower than from monofunctional P4VP-TTC, but triblock MW still increased linearly with St conversion. A low MW shoulder appeared in the GPC trace at St conversion > 40 %, which was ascribed to the different accessibility of the two RAFT termini to the monomer within the large *in situ* formed nano-objects. Similar morphology transitions were observed as in diblock copolymers, (i.e. spheres to worms, then vesicles), but additional large lacunal nanosphere morphologies were observed with the longest PSt blocks.

Hawker *et al.* expanded the field of aqueous RAFT dispersion polymerisations to synthesise thermoresponsive nano-gels.<sup>205</sup> PDMA-TTC was used as macro-RAFT for polymerisation of NIPAM at 70 °C, which could be cross-linked using MBA comonomer. By comparing two different macro-RAFT structures, one amphiphilic and one hydrophilic, they revealed that the macro-RAFT need not be amphiphilic in order to stabilise particles. Similarly, PEG-TTC was used in the copolymerisation of DEAA with MBA at 70 °C to yield a thermoresponsive nano-gel (PDEAA has an LCST at 32 °C).<sup>206</sup> Cao and An prepared biocompatible nanogels by using macro-RAFT agents with PEG backbones (PEG-TTC) or



PEG side chains (PPEGMA-TTC) for copolymerisation of DEGMA and PEGMA by RAFT dispersion polymerisation.<sup>207</sup>

### 3.c. RAFT Emulsion Polymerisation

As discussed in Section 2b, implementation of RAFT as an emulsion polymerisation is far from trivial,<sup>181,208</sup> and the addition of a low MW RAFT agent to an *ab initio* emulsion recipe typically yields problems with both colloidal stability and control/livingness. An early study succeeded in using a seeded emulsion approach, in which all RAFT agent was located in the preformed seed particles before polymerisation started, thus bypassing the problematic nucleation stage.<sup>209</sup> As with solvophobic block copolymer synthesis, Hawkett *et al.* first reported *ab initio* emulsion polymerisation using amphiphilic RAFT agents that self-assemble into micelles before polymerisation of the hydrophobic monomer (added using a feed technique to ensure absence of monomer droplets prior).<sup>168, 169, 210</sup> Chain extension of PAA-*b*-P<sup>n</sup>BuA-TTC with further <sup>n</sup>BuA under RAFT control produced PAA-*b*-P<sup>n</sup>BuA core-shell latex particles (~50 nm). Further studies using several low molecular weight PAA-*b*-PSt as macro-RAFT agents for *ab initio* emulsion polymerisation of St revealed that the key parameters for control of this system were diblock hydrophobicity and initiator concentration.<sup>210</sup>

Hydrophilic macro-RAFT agents were later exploited for *ab initio* emulsion polymerisation, and Rieger *et al.* adopted PEG-TTC for chain extension with St, <sup>n</sup>BuA or <sup>n</sup>BuA-*co*-MMA.<sup>170, 211</sup> Different lengths of PEG chain (1, 2, 5 kg mol<sup>-1</sup>) were found to affect the particle size and polymerisation kinetics, with longer PEG chains enhancing polymerisation rate and resulting in smaller particles. The best polymerisation control was achieved with PEG-2k, whilst PEG-1k resulted in multimodal MWD that was attributed to the heterogeneity of particle size, and PEG-5k resulted in larger  $\bar{D}$  (~1.4) due to a small amount of unfunctionalised PEG. The particle size could also be tuned by mixing PEG-TTC of different lengths, independent of the hydrophobic P<sup>n</sup>BuA block length. In a related study, pre-synthesised P4VP-TTC was chain extended with St-*co*-acrylonitrile (SAN) in aqueous emulsion polymerisation at low pH (4-5).<sup>91</sup> GPEC was used to confirm the complete transformation of the P4VP block into P4VP-*b*-SAN, i.e. quantitative blocking efficiency. Ji *et al.* reported the synthesis of amphiphilic polyacrylamide-*b*-PSt (PAAm-PSt) in what they referred to as batch emulsion polymerisation by using pre-synthesised PAAm-TTC as macro-RAFT.<sup>212</sup> However, an extra ultrasonication step was applied before starting the reaction at 75 °C, and as such it is clear that

this was actually a miniemulsion polymerisation. The authors hypothesised that the ultrasonication achieved smaller droplets which were then stabilised by PAAm chains to form initial particles in accordance with a miniemulsion mechanism.

A simple one-pot RAFT-controlled synthesis of amphiphilic block copolymers in water was reported by Chaduc *et al.* and Zhang *et al.* Using a trithiocarbonate RAFT agent, polymerisation of hydrophilic monomers (AA,<sup>213</sup> MAA or MAA-co-PEG<sub>18</sub>MA<sup>66</sup>) was first conducted to near full conversion, before St was added directly for chain extension and MW increased linearly with St conversion.<sup>213</sup> PAA-TTC showed the slowest reinitiation due to an unfavourable fragmentation of PAA at the early stage of polymerisation. In the case of PMAA-TTC (which is more hydrophobic than PAA), a shorter PSt block was required to impart amphiphilic properties and afford block copolymers which self-assemble. Thus, the compartmentalisation of polymerisation into St-swollen micelles occurred earlier, and as a result, blocking efficiency from PMAA-TTC and P(MAA-co-PEG<sub>18</sub>MA)-TTC was higher than from PAA-TTC. A kinetic study of P(MAA-co-PEG<sub>18</sub>MA)-*b*-PSt synthesis revealed that reorganisation of the particles during growth was a key step in the mechanism.<sup>66</sup> The number of particles as a function of monomer conversion decreased at low conversion (<20%) but remained constant at high conversion. Nucleation and growth of particles was governed by self-assembly of amphiphilic block copolymer chains (homogeneous nucleation) followed by adsorption of copolymer chains and/or coagulation/coalescence of already formed particles.

Non-spherical nano-objects can also be obtained by PISA from RAFT emulsion polymerisation under appropriate conditions.<sup>214-216</sup> The final morphology depends mainly on the target length of the hydrophobic block, in accordance with the overall **molecular packing parameter** (Fig. 2). A number of additional factors which favour the formation of non-spherical morphologies from amphiphilic block copolymers synthesised in RAFT emulsion polymerisation were first reported by Boissé *et al.*<sup>216</sup> Pre-synthesised P(AA-co-PEG<sub>7</sub>MA)-TTC was used to polymerise St in water at different salt concentrations and pH values. Lower pH or higher salt concentration drove the formation of nanofibers. At high pH, the acid groups of AA are mainly present in deprotonated ionic form. Repulsion between ionic PAA chains favours high curvature of core-corona interface, *i.e.* favours spherical objects, while fibers are more easily formed at low pH when some PAA groups are protonated. High salt concentration (*i.e.* high ionic strength) leads to charge screening, which minimises repulsions of charged carboxylates such that rods/vesicles can form. The morphology change from spheres to fibres

was observed as the PSt block grew. However, the final block copolymer had a broad molecular weight distribution ( $\mathcal{D} > 2$ ) and low monomer conversion ( $< 80\%$ ) in some cases.

The Charleux group also achieved non-spherical morphologies by substituting the comonomer AA in the macro-RAFT with MAA to achieve better control over St polymerisation.<sup>217</sup> Well-defined P(MAA-*co*-PEG<sub>18</sub>MA)-*b*-PSt was synthesised in a one-pot emulsion polymerisation in water at pH 5, although first block synthesis was conducted at pH 3.5. High conversion ( $> 95\%$ ) was achieved in  $\sim 5$  h and the final block copolymer had low  $\mathcal{D}$  ( $< 1.5$ ). As with the PAA macro-RAFT, pH was one of the critical parameters when targeting non-spherical structures, since only spheres were obtained at pH 3.5.<sup>66</sup> The morphology change from spheres, to nanofibers and vesicles was observed during PSt block growth, which was plotted in a phase diagram against DP of hydrophobic PSt block and hydrophilic P(MAA-*co*-PEG<sub>18</sub>MA) block (Fig. 14).

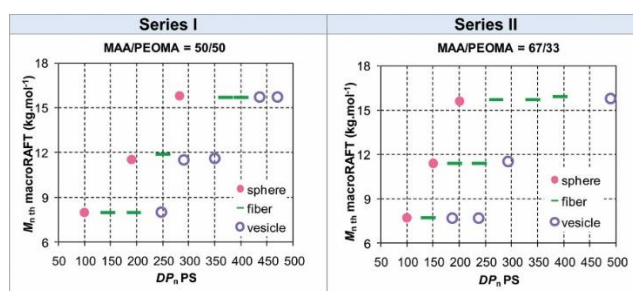


**Figure 14:** The phase diagram for aqueous emulsion polymerisation of styrene using P(MAA-*co*-PEG<sub>18</sub>MA) as macro-RAFT. Morphology transitions from spheres, to nanofibers and vesicles were clearly observed during PSt block growth. Adapted with permission from Ref.<sup>217</sup>, copyright ACS, 2012.

Rapid synthesis of ultrahigh MW PSt-containing diblock copolymers by RAFT emulsion polymerisation was reported by Truong *et al.*<sup>218</sup> A novel macro-RAFT agent based on N-hydroxyethyl acrylamide (HEAA) and PEGA (PHEAA-*co*-PPEGA-TTC) was pre-synthesised and chain extended with St. Ultrahigh MW block copolymers (up to  $10^6$  g mol<sup>-1</sup>) with low  $\mathcal{D}$  ( $< 1.4$ ) were achieved in 6 h and the final particles had narrow size distribution. In a later study by the group, low toxicity block copolymers were prepared using P(DEGMA-*co*-HPMA)-TTC for polymerisation of St,<sup>219</sup> from which multiple morphologies were achieved by adjusting the block ratio and length, although additional surfactant (SDS) was used.

### 3.d. NMP in emulsion/dispersion

The initial studies by the Charleux group on nitroxide-mediated emulsion/dispersion polymerisation were based on a water-soluble poly(sodium acrylate) alkoxyamine macroinitiator (PNaA-SG1).<sup>220-222</sup> Amphiphilic block copolymers PAA-*b*-PSt or PAA-*b*-P<sup>n</sup>BuA were prepared in water using a PNaA-SG1 at 120 °C. A stable emulsion of spherical nanoparticles was obtained through PISA as the hydrophobic block grew.<sup>221</sup> The kinetics of PAA-*b*-PSt prepared in *ab initio* emulsion polymerisation mediated by PNaA-SG1 suggested an influence of the compartmentalisation of propagating radicals on the polymerisation rate.<sup>222, 223, 224</sup> Notably, the polymerisation proceeded in a controlled manner even at a high solids content (39%).

Thermo-responsive nanogels of PNaA-*b*-PDEAA were prepared by using PNaA-SG1 and a small amount of free nitroxide SG1 (<10 mol%)<sup>225</sup> to lower the rate of DEAA polymerisation and improve control by more rapidly establishing the persistent radical effect.<sup>158</sup> DEAA polymerisation exhibited good control/livingness at different temperatures (112 and 120 °C) and solids contents (20 – 39 wt%),<sup>158</sup> and MBA (<3% of DEAA) was added after 1h of reaction to cross-link the PDEAA core during chain extension whilst avoiding macrogelation.<sup>225</sup> The group also revealed that PMAA-SG1 showed a higher initiating efficiency than PAA-SG1 when chain extending with MMA or St,<sup>171, 172</sup> a result that is parallel to findings with the analogous macro-RAFT agents.<sup>213, 66</sup> However, the co-monomers St<sup>171</sup> or sodium 4-styrene sulfonate (SS)<sup>172</sup> (~ 10 mol%) were necessary to achieve controlled synthesis of PMAA-SG1, a well-known strategy for NMP of methacrylates.<sup>226, 227</sup>

Non-spherical block copolymer nano-objects can also be obtained by nitroxide-mediated emulsion polymerisation. This was achieved during the one-pot synthesis of PAA-*b*-P4VP,<sup>228</sup> in which PNaA<sub>21</sub>-SG1 was first synthesised in water at 120 °C and pH 11, and then used as the initiator for controlled polymerisation of 4VP under the same conditions (at which 4VP and P4VP were insoluble). High conversion (98 %) was attained in just 2 h, and polymerisation was fairly well-controlled ( $\bar{D} = 1.65$ ). Pure spheres evolved into pure vesicles ( $d < 500$  nm) as the P4VP block grew, although the vesicles had a broad size distribution. Groison *et al.* also synthesised amphiphilic block copolymer nano-fibres and vesicles by nitroxide-mediated emulsion polymerisation of MMA/St (91:9, mol/mol), using a pre-synthesised P(MAA<sub>41</sub>-*co*-SS<sub>10</sub>)-SG1.<sup>229</sup> As the hydrophobic block grew, spheres transformed into fibres and then vesicles (Fig. 15), and block copolymer dispersity remained at 1.2 – 1.4.

Cunningham's group explored macroinitiators beyond the ubiquitous PAA- or PMAA-SG1, instead adopting tertiary amine-containing and pH-responsive macro-initiators, PDMAEMA-SG1 and poly(N,N-diethylaminoethyl methacrylate) (PDEAEMA)-SG1.<sup>230, 231</sup> They exploited one-pot emulsion polymerisation of MMA/St (90/10, mol/mol) using P(DEAEMA-*co*-St)-SG1 as macroalkoxyamine.<sup>230</sup> The MW increased linearly with monomer conversion (>80% conversion in 5 h) and  $\bar{D}$  remained relatively low (<1.5).

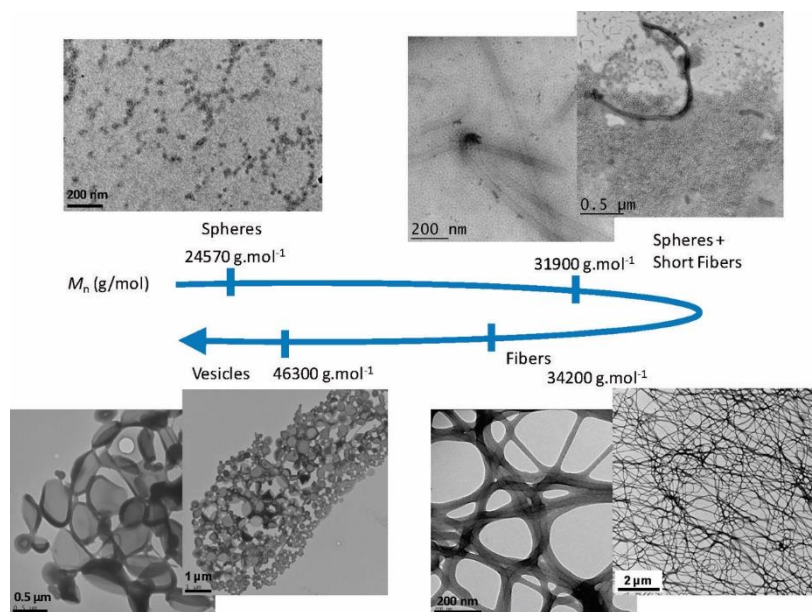


**Figure 15:** TEM images for the nano-objects obtained during nitroxide-mediated emulsion polymerisation of MMA/St (91:9, mol/mol) using P(MAA-*co*-SS)-SG1 as macroalkoxyamine. Morphology transitions from spheres, to nanofibers and vesicles were clearly observed during the hydrophobic block growth. Reprinted with permission from Ref. <sup>229</sup>, copyright ACS, 2012.

### 3.e. Other CLRP in emulsion

Okubo and co-workers explored TERP for amphiphilic block copolymer synthesis under emulsion conditions, starting with a water-soluble macroTERP agent, typically PMAA-TeMe.<sup>127, 232-239</sup> This approach was successfully applied for St, <sup>n</sup>BuA, and MMA. Adopting a high stirring rate and low temperature had a favourable influence over control/livingness and particle size distribution. At a higher stirring rate (1000 rpm) the St phase was dispersed as droplets, and well-defined PMAA-*b*-PSt nanoparticles of small size ( $d \sim 50$  nm) were achieved, while low stirring rate led to bimodal particle size distribution.<sup>232, 234</sup> The initial rate of

consumption of the initial macro-TERP agent increased at higher stirring rate, which resulted in an increased number of particles of smaller diameter.<sup>235</sup> A follow up study used PDMAEMA-butyltelleanyl (PDMAEMA-TeBu) as macro-TERP in emulsion polymerisation of St,<sup>238</sup> and found that the chain length of macro-TERP affected the particle size and MWD control. A short PDMAEMA-TeBu chain afforded better MWD control and smaller particles, while a long chain length delayed the self-assembly nucleation, resulting in homogeneous nucleation and poor MWD control.

Very recently, PPEGMA-*b*-PSt and PPEGMA-*b*-PMMA were synthesised in one-pot in an aqueous emulsion process using copper(II) acetate as a catalyst and a dithiocarbamate as the hydrophilic initiator.<sup>240</sup> PPEGMA macroinitiator was first synthesised in water with narrow  $\bar{D}$  (<1.3), before MMA or St were added sequentially. A shorter PPEGMA macroinitiator resulted in better control over PPEGMA-*b*-PMMA synthesis ( $\bar{D} = 1.15$ ) but with a relatively broad particle size distribution (of spherical particles), which contrasts with the results from TERP-controlled synthesis above.

### 3.f. Amphiphilic block copolymer synthesis: Discussion

The synthesis of amphiphilic polymeric materials by combining the advantages of hetero-phase polymerisation (producing materials ready for use without purification) and CLRP (MW and dispersity control) could be ideal for an industrial setting. The research summarised above is dominated by procedures adopting *ab initio* emulsion and dispersion, which are simple and industrially-relevant techniques, although seeded emulsion mechanisms have also shown promise. To simultaneously achieve control over polymerisation and colloidal stability, the use of a macro-RAFT or macro-initiators comprising homopolymer or amphiphilic block copolymer is an established strategy. However, to circumvent the need for an additional step, research groups have developed one-pot procedures in which the solvophilic block is synthesised *in situ* before the addition of hydrophobic monomer.<sup>65, 66, 174, 175, 190, 195, 197, 213, 217, 230</sup> Dispersion CLRP synthesis of amphiphilic block copolymers is an attractive approach due to the initially homogeneous conditions, but the range of monomers applicable under aqueous conditions is limited. Dispersion polymerisation in non-aqueous solvents such as cyclohexane,<sup>173</sup> chloroform<sup>191</sup> and methanol.<sup>174, 192-194</sup> have enabled the synthesis of amphiphilic polymers with a broad spectrum of solubility properties and structures, but adversely require VOCs.

Of all CLRP-controlled syntheses of amphiphilic block copolymers, the majority of reports adopt RAFT, due in part to high aqueous stability of the CTA and its operation under low temperature conditions. Furthermore, the degenerative chain transfer mechanism ensures the RAFT agent remains attached to the polymer chain at all stages and minimises partitioning between phases (in contrast to copper (II) species in ATRP or SG1 in NMP). The recent development of successful TERP synthesis of amphiphilic block copolymers under emulsion conditions somewhat confirms that this degenerative chain transfer mechanism is widely applicable to heterogeneous conditions.

In the last 10 years, interest in synthesis of amphiphilic block copolymer nano-objects from heterogeneous polymerisations has been driven by the discovery of various morphologies including spherical micelles, worm-like micelles, and vesicles that are obtained by self-assembly as the polymerisations proceeds (Fig. 2). The morphologies are somewhat predictable (by considering the molecular packing parameter), and are dictated by the nature of the amphiphilic block copolymers as well as the polymerisation conditions. The discovery of non-spherical morphologies was a particular breakthrough, as this expanded the potential range of functional materials accessible. One of the key universal factors in targeting these non-spherical morphologies is that the glass transition temperature ( $T_g$ ) of the core phase needs to be sufficiently low to allow chain reorganisation from spheres to other more complex morphologies. The size and shape of nano-objects can be tuned by parameters including i) the length of the hydrophilic block (macroinitiator in NMP and ATRP, or macro-RAFT agent), ii) the length of the hydrophobic block, iii) the overall solids content, iv) continuous phase pH (in aqueous systems), and v) salt concentration.

There are a number of future challenges to be undertaken in this field in order to move towards material applications, in particular the development of routes to assemblies with monodisperse sizes and pure morphologies. This is especially true for worm-like micelles or nanofibers, which have very large aspect ratios and are promising for applications in materials science, but the phase window (i.e. range of conditions for their formation) is very narrow. More complex morphologies are also desired, such as the intermediate phases observed by Armes and co-workers.<sup>157, 176, 177</sup> Furthermore, there is increasing attention toward cross-linking polymers during amphiphilic block copolymer synthesis to lock-in morphologies and afford nano/microgels and macrohydrogels with responsive properties.<sup>205-207, 225</sup>

#### **4. Conclusions and future outlook**

In this article, we have reviewed the numerous promising ways by which to prepare block copolymer particles by CLRP in dispersed systems. It is necessary to highlight at this point that there are alternative routes to block copolymer particles that have also been explored. Solvophobic block copolymer particles can be prepared by numerous techniques, which are thoroughly reviewed elsewhere,<sup>241-243</sup> including: 1) self-organised reprecipitation (SORP), in which particles precipitate upon solvent evaporation from a solution of block copolymer in a non-solvent/solvent mixture<sup>151, 244, 245</sup>; 2) evaporation-induced self-assembly (EISA), where a polymer dissolved in a non-polar solvent is dispersed in water, and solvent evaporation leads to block copolymer self-assembly<sup>246-248</sup>; 3) solvent evaporation from block copolymer aerosols; 4) templating within the pores of inverse opals<sup>249</sup>; and 5) precipitation from a good solvent mixture into a poor solvent.<sup>250, 251</sup> Although these routes are becoming well-established they require multiple steps, from the synthesis of block copolymer (often by anionic polymerisation) to the preparation of precursor solutions and time-consuming solvent evaporation. Amphiphilic block copolymer nano-objects are usually prepared by dispersing the copolymers in aqueous media, either by dialysis from a cosolvent,<sup>252</sup> precipitation into water,<sup>253</sup> or directly rehydrating the solid.<sup>254</sup> These processes typically yield low concentrations of nano-objects (<1 wt%), whilst CLRP in dispersed systems can advantageously be prepared in high concentration or solid content (up to 40 wt%).

Clearly, CLRP in dispersed systems can provide a much simplified and potentially commercial route to block copolymer particles where synthesis and self-assembly take place (in many cases) in one pot. CLRP in dispersed systems results in polymer particles dispersed in solvent that may be ready for further application, or to be processed into other form factors. Bulk block copolymers already enjoy significant commercial success in rubbers, adhesives, tires and surfactants (to name a few), but are usually synthesised by anionic polymerisation. Dispersed CLRP could provide an alternative route to block copolymers with similar properties, thus allowing access to the same applications (as already demonstrated for thermoplastic elastomers<sup>107, 115</sup>) *via* a route that has financial and environmental advantages. Furthermore, these synthetic approaches can allow access to kinetically-trapped structures<sup>138</sup> and novel morphologies that are difficult or impossible to achieve otherwise, e.g. worm-like micelles from amphiphilic block copolymers.<sup>81, 157, 177, 178, 217 117</sup>

The use of block copolymer particles as functional materials is a field still in its infancy, but has been gathering interest over the last 5 years and could broaden the overall scope of block copolymer applications by orders of magnitude. Amphiphilic block copolymer particles



synthesised by CLRP have already been investigated in drug delivery,<sup>255, 256</sup> sensors,<sup>257</sup> Pickering emulsifiers,<sup>258</sup> gels for cell growth<sup>259</sup> and coatings,<sup>260</sup> and these nano-objects could further impact on diverse fields including nanoreactors,<sup>261</sup> theranostics,<sup>262</sup> and the controlled synthesis of inorganic NPs.<sup>263, 264</sup> Larger block copolymer particles (*i.e.* in which particle size is much greater than the length scale of the block copolymer) with internal nanostructure, such as those obtained in solvophobic block copolymer synthesis, are being studied in diverse applications, including: drug delivery vehicles, in which drug release can be triggered by degradation of one block<sup>265, 266</sup> or a change in temperature<sup>267-269</sup>; diagnostics<sup>268</sup>; hydrogel actuators<sup>270</sup>; and impact modifiers to toughen polymeric materials.<sup>117, 271-273</sup> Indeed, further processing of nanostructured block copolymer particles (*i.e.* through lithographic degradation) can afford porous particles for protein separation or drug delivery (Fig. 16),<sup>250</sup> chromatographic columns, and catalyst supports. The wider applicability of nanostructured particles based on block copolymers has been demonstrated through loading with inorganic nanoparticles (e.g. gold,<sup>274</sup> platinum<sup>275</sup> and quantum dots,<sup>276</sup> Fig. 17) which could ultimately lead to exciting new opportunities in catalysis, sensors, optoelectronics, plasmonics,<sup>277</sup> and photonics.<sup>278</sup> Block copolymer particles have previously been exploited as templates for mesoporous inorganic particles<sup>279</sup> with potential in photovoltaic devices.<sup>280</sup>

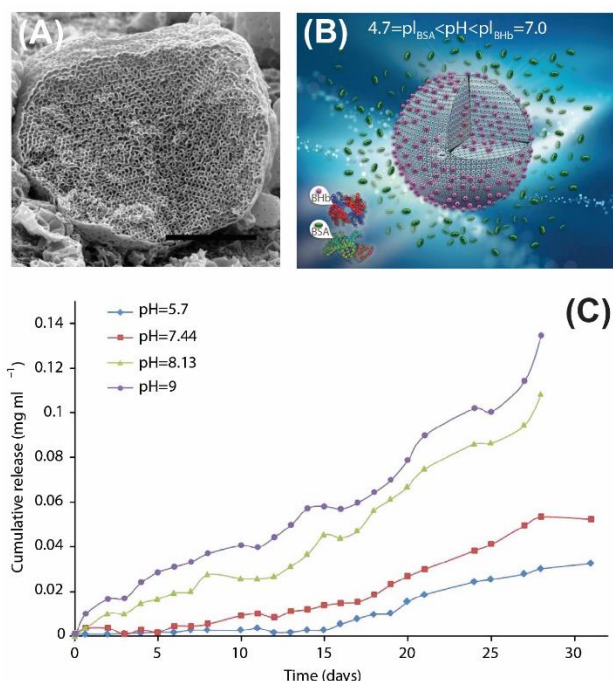


**Figure 16:** Application of porous block copolymer particles (based on PSt-b-PAA) in selective protein separation under pH-dependent conditions. (A) Cross-sectional SEM image of fractured block copolymer particle demonstrating the regular pores arising from block

copolymer self-assembly (scale bar = 1  $\mu\text{m}$ ). (B) Schematic demonstrating the separation of proteins with similar sizes (green and red) using the porous particles. (C) Plot illustrating the sustained release of protein over time at different pH values. Adapted with permission from reference <sup>250</sup>, copyright Nature Publishing Group, 2014.

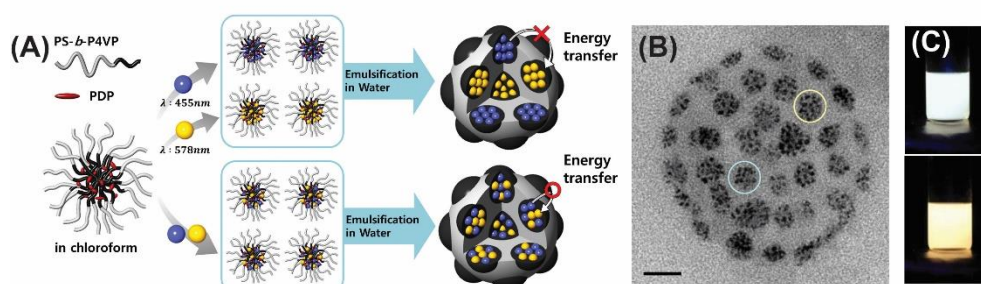


**Figure 17:** (A) Loading of quantum dots (QDs) into PSt-b-P4VP block particles enables the tuning of light emission, depending on whether differently-sized QDs are loaded into different domains, or mixed within the same domain. (B) Cross-sectional TEM image demonstrating the localisation of QDs to the P4VP cores, and their separation into different compartments (scale bar = 50nm). (C) Image of block copolymer particle dispersions in which the two types of QDs are in separate domains (top) or mixed in the same domain (bottom), indicating the tuneable emission properties. Adapted with permission from reference <sup>276</sup>, copyright Wiley, 2013.

Accessing this diverse range of potential applications for block copolymer particles necessitates a modular, scalable approach to synthesise block copolymers with desired functionality and particles with controlled size and internal morphology. The understanding of synthesis and *in situ* self-assembly of block copolymers *via* CLRP in dispersed systems is advancing, but the future of block copolymer particles with real-world applications relies on the adaptability of processes to a range of monomers with different reactivity and functionality, the employment of relatively benign conditions and environmentally-friendly solvents, and reproducibility of nanoscale morphology based on block copolymer composition and reaction environment.

## References

1. R. G. Gilbert, *Emulsion Polymerization: A Mechanistic Approach*, Academic Press, London, 1995.
2. S. C. Thickett and R. G. Gilbert, *Polymer*, 2007, 48, 6965-6991.
3. J. M. Asua, *Prog. Polym. Sci.*, 2002, 27, 1283.
4. J. M. Asua, *Prog. Polym. Sci.*, 2014, 39, 1797-1826.
5. M. Antonietti and K. Landfester, *Prog. Polym. Sci.*, 2002, 27, 689-757.
6. F. Candau, in *Polymeric dispersions: Principles and applications*, ed. J. M. Asua, Kluwer Academic Publishers, 1997, pp. 127-140.
7. P. Y. Chow and L. M. Gan, *Adv. Polym. Sci.*, 2005, 175, 257-298.
8. P. B. Zetterlund, F. Aldabbagh and M. Okubo, *Journal of Polymer Science Part a-Polymer Chemistry*, 2009, 47, 3711-3728.
9. K. E. J. Barrett, *Brit. Polym. J.*, 1973, 5, 259-271.
10. J. L. Cawse, in *Emulsion Polymerization and Emulsion Polymers*, eds. P. A. Lovell and M. S. El-Aasser, John Wiley & Sons Ltd., West Sussex, 1997, pp. 743-761.
11. A. P. Richez, H. N. Yow, S. Biggs and O. J. Cayre, *Progress in Polymer Science*, 2013, 38, 897-931.
12. R. Arshady, *Colloid Polym. Sci.*, 1992, 270, 717-732.
13. I. Capek, *Adv. Colloid Interface Sci.*, 2010, 156, 35-61.
14. P. B. Zetterlund, F. Aldabbagh and M. Okubo, *J. Polym. Sci.; Part A: Polym. Chem.*, 2009, 47, 3711-3728.
15. K. J. Thurecht and S. M. Howdle, *Aust. J. Chem.*, 2009, 62, 786-789.
16. J. L. Kendall, D. A. Canelas, J. L. Young and J. M. DeSimone, *Chem. Rev.*, 1999, 99, 543-563.
17. P. B. Zetterlund, Y. Kagawa and M. Okubo, *Chem. Rev.*, 2008, 108, 3747-3794.
18. A. D. Jenkins, R. G. Jones and G. Moad, *Pure and Applied Chemistry*, 2010, 82, 483-491.
19. P. Taylor, *Adv. Colloid Interface Sci.*, 1998, 75, 107-163.
20. A. Goto and T. Fukuda, *Prog. Polym. Sci.*, 2004, 29, 329-385.
21. J. Nicolas, Y. Guillaneuf, C. Lefay, D. Bertin, D. Gigmes and B. Charleux, *Prog. Polym. Sci.*, 2013, 38, 63-235.
22. K. Matyjaszewski, *Macromolecules*, 2012, 45, 4015-4039.
23. G. Moad, E. Rizzardo and S. H. Thang, *Aust. J. Chem.*, 2012, 65, 985-1076.
24. M. Szwarc, M. Levy and R. Milkovich, *J. Am. Chem. Soc.*, 1956, 78, 2656-2657.
25. J.-F. Lutz, M. Ouchi, D. R. Liu and M. Sawamoto, *Science*, 2013, 341, 628-637.
26. A. H. Soeriyadi, C. Boyer, F. Nystrom, P. B. Zetterlund and M. R. Whittaker, *J. Am. Chem. Soc.*, 2011, 133, 11128-11131.
27. C. Boyer, A. H. Soeriyadi, P. B. Zetterlund and M. R. Whittaker, *Macromolecules*, 2011, 44, 8028-8033.
28. A. Anastasaki, C. Waldron, P. Wilson, C. Boyer, P. B. Zetterlund, M. R. Whittaker and D. Haddleton, *ACS Macro Letters*, 2013, 2, 896-900.
29. D. Konkolewicz, Y. Wang, P. Krysz, M. Zhong, A. A. Isse, A. Gennaro and K. Matyjaszewski, *Polym. Chem.*, 2014, 5, 4396-4417.
30. B. M. Rosen and V. Percec, *Chem. Rev.*, 2009, 109, 5069-5119.
31. G. Gody, T. Maschmeyer, P. B. Zetterlund and S. Perrier, *Macromolecules*, 2014, 47, 639-649.
32. P. B. Zetterlund, G. Gody and S. Perrier, *Macromol. Theory Simul.*, 2014, 23, 331-339.
33. G. Gody, T. Maschmeyer, P. B. Zetterlund and S. Perrier, *Macromolecules*, 2014, 47, 3451-3460.
34. J. Vandenbergh, T. d. m. Ogawa and T. Junkers, *J. Polym. Sci.; Part A: Polym. Chem.*, 2013, 51, 2366-2374.
35. G. Gody, P. B. Zetterlund, S. Perrier and S. Harrisson, *Nature communications*, 2016, 7, 10514-10514.
36. G. Gody, T. Maschmeyer, P. B. Zetterlund and S. Perrier, *Nature Communications*, 2013, 4.
37. W. A. Braunecker and K. Matyjaszewski, *Prog. Polym. Sci.*, 2007, 32, 93-146.
38. K. Matyjaszewski and N. V. Tsarevsky, *J. Am. Chem. Soc.*, 2014, 136, 6513-6533.

39. A. Gregory and M. H. Stenzel, *Progress in Polymer Science*, 2012, 37, 38-105.
40. J. Qiu, B. Charleux and K. Matyjaszewski, *Prog. Polym. Sci.*, 2001, 26, 2083-2134.
41. M. F. Cunningham, *Prog. Polym. Sci.*, 2002, 27, 1039-1067.
42. M. F. Cunningham, *C. R. Chimie*, 2003, 6, 1351-1374.
43. M. J. Monteiro and B. Charleux, in *Chemistry and Technology of Emulsion Polymerization*, ed. A. M. v. Herk, Blackwell Publishing Ltd., Oxford, 2005, pp. 111-139.
44. F. J. Schork, Y. W. Luo, W. Smulders, J. P. Russum, A. Butte and K. Fontenot, *Adv. Polym. Sci.*, 2005, 175, 129-255.
45. J. B. McLeary and B. Klumperman, *Soft Matter*, 2006, 2, 45-53.
46. M. Save, Y. Guillauneuf and R. G. Gilbert, *Aust. J. Chem.*, 2006, 59, 693-711.
47. M. F. Cunningham, *Prog. Polym. Sci.*, 2008, 33, 365-398.
48. J. K. Oh, *J. Polym. Sci.; Part A: Polym. Chem.*, 2008, 46, 6983-7001.
49. K. Min and K. Matyjaszewski, *Central Eur. J. Chem.*, 2009, 7, 657-674.
50. P. B. Zetterlund, Y. Kagawa and M. Okubo, *Chemical Reviews*, 2008, 108, 3747-3794.
51. P. B. Zetterlund, S. C. Thickett, S. Perrier, E. Bourgeat-Lami and M. Lansalot, *Chemical Reviews*, 2015, 115, 9745-9800.
52. M. J. Monteiro and M. F. Cunningham, *Macromolecules*, 2012, 45, 4939-4957.
53. J. K. Oh, C. Tang, H. Gao, N. V. Tsarevsky and K. Matyjaszewski, *J. Am. Chem. Soc.*, 2006, 128, 5578-5584.
54. M. A. M. Oliveira, C. Boyer, M. Nele, J. C. Pinto, P. B. Zetterlund and T. P. Davis, *Macromolecules*, 2011, 44, 7167-7175.
55. P. B. Zetterlund, S. C. Thickett, S. Perrier, E. Bourgeat-Lami and M. Lansalot, *Chem. Rev.*, 2015.
56. K. Landfester, *Angew. Chem.-Int. Edit.*, 2009, 48, 4488-4507.
57. Y. Luo, J. Tsavalas and F. J. Schork, *Macromolecules*, 2001, 34, 5501-5507.
58. L. Yang, Y. Luo and B. Li, *Polymer*, 2006, 47, 751-762.
59. Y. Guo, J. Q. Liu and P. B. Zetterlund, *Macromolecules*, 2010, 43, 5914-5916.
60. U. El-Jaby, M. Cunningham and T. F. L. McKenna, *Macromol. Rapid Commun.*, 2010, 31, 558-562.
61. S. Q. Cheng, S. R. S. Ting, F. P. Lucien and P. B. Zetterlund, *Macromolecules*, 2012, 45, 1803-1810.
62. H. Maehata, X. Liu, M. Cunningham and B. Keoshkerian, *Macromol. Rapid Commun.*, 2008, 29, 479-484.
63. M. Chenal, L. Bouteiller and J. Rieger, *Polym. Chem.*, 2013, 4, 752-762.
64. I. Chaduc, A. Crepet, O. Boyron, B. Charleux, F. D'Agosto and M. Lansalot, *Macromolecules*, 2013, 46, 6013-6023.
65. I. Chaduc, M. Girod, R. Antoine, B. Charleux, F. D'Agosto and M. Lansalot, *Macromolecules*, 2012, 45, 5881-5893.
66. W. J. Zhang, F. D'Agosto, O. Boyron, J. Rieger and B. Charleux, *Macromolecules*, 2011, 44, 7584-7593.
67. C. J. Ferguson, R. J. Hughes, B. T. T. Pham, B. S. Hawkett, R. G. Gilbert, A. K. Serelis and C. H. Such, *Macromolecules*, 2002, 35, 9243-9245.
68. C. J. Ferguson, R. J. Hughes, D. Nguyen, B. T. T. Pham, R. G. Gilbert, A. K. Serelis, C. H. Such and B. S. Hawkett, *Macromolecules*, 2005, 38, 2191-2204.
69. E. Sprong, J. S. Leswin, D. J. Lamb, C. J. Ferguson, B. S. Hawkett, B. T. Pham, D. Nguyen, C. H. Such, A. K. Serelis and R. G. Gilbert, *Macromol. Symp.*, 2006, 231, 84-93.
70. B. Charleux and J. Nicolas, *Polymer*, 2007, 48, 5813-5833.
71. G. Delaittre, J. Nicolas, C. Lefay, M. Save and B. Charleux, *Chem. Commun.*, 2005, 5, 614-616.
72. Y. Kagawa, P. B. Zetterlund, H. Minami and M. Okubo, *Macromolecules*, 2007, 40, 3062-3069.
73. A. M. Elsen, J. Burdynska, S. Park and K. Matyjaszewski, *Macromolecules*, 2012, 45, 7356-7363.
74. S. Y. Liu, K. D. Hermanson and E. W. Kaler, *Macromolecules*, 2006, 39, 4345-4350.
75. P. B. Zetterlund and M. Okubo, *Macromolecules*, 2006, 39, 8959-8967.
76. P. B. Zetterlund, *Polym. Chem.*, 2011, 2, 534-549.

77. T. Nakamura, P. B. Zetterlund and M. Okubo, *Macromol. Rapid Commun.*, 2006, 27, 2014-2018.
78. P. B. Zetterlund, T. Nakamura and M. Okubo, *Macromolecules*, 2007, 40, 8663-8672.
79. J.-S. Song and M. A. Winnik, *Macromolecules*, 2006, 39, 8318-8325.
80. B. Charleux, G. Delaittre, J. Rieger and F. D'Agosto, *Macromolecules*, 2012, 45, 6753-6765.
81. W.-M. Wan, C.-Y. Hong and C.-Y. Pan, *Chem. Commun.*, 2009, DOI: 10.1039/B912804B, 5883-5885.
82. J.-T. Sun, C.-Y. Hong and C.-Y. Pan, *Polym. Chem.*, 2013, 4, 873-881.
83. N. J. Warren and S. P. Armes, *J. Am. Chem. Soc.*, 2014, 136, 10174-10185.
84. J. T. Sun, C. Y. Hong and C. Y. Pan, *Soft Matter*, 2012, 8, 7753-7767.
85. I. Tausendfreund, F. Bandermann, H. W. Siesler and M. Kleimann, *Polymer*, 2002, 43, 7085-7091.
86. J. Kim, S. Y. Jeong, K. U. Kim, Y. H. Ahn and R. P. Quirk, *Journal of Polymer Science Part a-Polymer Chemistry*, 1996, 34, 3277-3288.
87. Y. Kitayama, M. Yorizane, H. Minami and M. Okubo, *Polymer Chemistry*, 2012, 3, 1394-1398.
88. J.-A. Raust, L. Houillot, M. Save, B. Charleux, C. Moire, C. Farcet and H. Pasch, *Macromolecules*, 2010, 43, 8755-8765.
89. M. J. Monteiro and J. de Barbeyrac, *Macromolecules*, 2001, 34, 4416-4423.
90. M. Semsarilar, E. R. Jones and S. P. Armes, *Polymer Chemistry*, 2014, 5, 195-203.
91. J. Bozovic-Vukic, H. T. Manon, J. Meuldijk, C. Koning and B. Klumperman, *Macromolecules*, 2007, 40, 7132-7139.
92. K. Min, H. F. Gao and K. Matyjaszewski, *Journal of the American Chemical Society*, 2006, 128, 10521-10526.
93. M. Okubo, H. Minami and J. Zhou, *Colloid Polym. Sci.*, 2004, 282, 747-752.
94. Y. Kagawa, H. Minami, M. Okubo and H. Zhou, *Polymer*, 2005, 46, 1045-1049.
95. Y. Kitayama, M. Yorizane, Y. Kagawa, H. Minami, P. B. Zetterlund and M. Okubo, *Polymer*, 2009, 50, 3182-3187.
96. Y. Kitayama, Y. Kagawa, H. Minami and M. Okubo, *Langmuir*, 2010, 26, 7029-7034.
97. J. Shu, C. Cheng, Y. Zheng, L. Shen, Y. Qiao and C. Fu, *Polymer Bulletin*, 2011, 67, 1185-1200.
98. Z. Xue, Z. Wang, D. He, X. Zhou and X. Xie, *Journal of Polymer Science Part a-Polymer Chemistry*, 2016, 54, 611-620.
99. J. K. Oh, F. Perineau and K. Matyjaszewski, *Macromolecules*, 2006, 39, 8003-8010.
100. B. Grignard, C. Jerome, C. Calberg, R. Jerome, W. X. Wang, S. M. Howdle and C. Detrembleur, *Macromolecules*, 2008, 41, 8575-8583.
101. H. Minami, A. Tanaka, Y. Kagawa and M. Okubo, *Journal of Polymer Science Part a-Polymer Chemistry*, 2012, 50, 2578-2584.
102. M. J. Monteiro, M. Sjoberg, J. van der Vlist and C. M. Gottgens, *Journal of Polymer Science Part a-Polymer Chemistry*, 2000, 38, 4206-4217.
103. W. Smulders and M. J. Monteiro, *Macromolecules*, 2004, 37, 4474-4483.
104. S. Pascual, C. N. Urbani and M. J. Monteiro, *Macromolecular Reaction Engineering*, 2010, 4, 257-263.
105. W. W. Smulders, C. W. Jones and F. J. Schork, *Macromolecules*, 2004, 37, 9345-9354.
106. A. Bowes, J. B. McLeary and R. D. Sanderson, *Journal of Polymer Science Part a-Polymer Chemistry*, 2007, 45, 588-604.
107. Y. W. Luo, X. G. Wang, Y. Zhu, B. G. Li and S. P. Zhu, *Macromolecules*, 2010, 43, 7472-7481.
108. Y. Guo, X. Gao and Y. Luo, *Journal of Polymer Science Part a-Polymer Chemistry*, 2015, 53, 1464-1473.
109. Y. Guo, J. Zhang, P. Xie, X. Gao and Y. Luo, *Polymer Chemistry*, 2014, 5, 3363-3371.
110. X. Zhan, R. He, Q. Zhang and F. Chen, *Rsc Advances*, 2014, 4, 51201-51207.
111. L. Yang, P. Sun, H. Yang, D. Qi and M. Wu, *Progress in Organic Coatings*, 2014, 77, 305-314.
112. J. Yang, Y. Bao and P. Pan, *Journal of Applied Polymer Science*, 2014, 131.
113. R. Z. Wei, Y. W. Luo and Z. S. Li, *Polymer*, 2010, 51, 3879-3886.

114. R. Wei, Y. Luo and P. Xu, *Journal of Polymer Science Part a-Polymer Chemistry*, 2011, 49, 2980-2989.
115. R. Wei, Y. Luo, W. Zeng, F. Wang and S. Xu, *Industrial & Engineering Chemistry Research*, 2012, 51, 15530-15535.
116. P. Froimowicz, B. van Heukelum, C. Scholten, K. Greiner, O. Araujo and K. Landfester, *Journal of Polymer Science Part a-Polymer Chemistry*, 2014, 52, 883-889.
117. Y. Zhu, X. Gao and Y. W. Luo, *Journal of Applied Polymer Science*, 2016, 133.
118. A. Sogabe and C. L. McCormick, *Macromolecules*, 2009, 42, 5043-5052.
119. J. Jennings, M. Beija, A. P. Richez, S. D. Cooper, P. E. Mignot, K. J. Thurecht, K. S. Jack and S. M. Howdle, *Journal of the American Chemical Society*, 2012, 134, 4772-4781.
120. J. Jennings, M. Beija, J. T. Kennon, H. Willcock, R. K. O'Reilly, S. Rimmer and S. M. Howdle, *Macromolecules*, 2013, 46, 6843-6851.
121. G. Hawkins, P. B. Zetterlund and F. Aldabbagh, *Journal of Polymer Science Part a-Polymer Chemistry*, 2015, 53, 2351-2356.
122. J. Nicolas, A. V. Ruzette, C. Farcet, P. Gerard, S. Magnet and B. Charleux, *Polymer*, 2007, 48, 7029-7040.
123. T. E. Enright, M. F. Cunningham and B. Keoshkerian, *Macromolecular Reaction Engineering*, 2010, 4, 186-196.
124. P. O'Connor, R. B. Yang, W. M. Carroll, Y. Rochev and F. Aldabbagh, *Eur. Polym. J.*, 2012, 48, 1279-1288.
125. Y. Fuji, T. Ando, M. Kamigaito and M. Sawamoto, *Macromolecules*, 2002, 35, 2949-2954.
126. J. Tonnar, P. Lacroix-Desmazes and B. Boutevin, *Macromolecules*, 2007, 40, 6076-6081.
127. Y. Kitayama, K. Kishida, H. Minami and M. Okubo, *J Polym Sci Pol Chem*, 2012, 50, 1991-1996.
128. T. Kuroda, T. Taniyama, Y. Kitayama and M. Okubo, *Macromolecules*, 2015, 48, 2473-2479.
129. A. Kermagoret, C. Ngoc Do Quyen, B. Grignard, D. Cordella, A. Debuigne, C. Jerome and C. Detrembleur, *Macromolecular Rapid Communications*, 2016, 37, 539-544.
130. M. Li, N. M. Jahed, K. Min and K. Matyjaszewski, *Macromolecules*, 2004, 37, 2434-2441.
131. K. Min, H. F. Gao and K. Matyjaszewski, *Journal of the American Chemical Society*, 2005, 127, 3825-3830.
132. C. J. Ferguson, R. J. Hughes, D. Nguyen, B. T. T. Pham, R. G. Gilbert, A. K. Serelis, C. H. Such and B. S. Hawkett, *Macromolecules*, 2005, 38, 2191-2204.
133. E. Sprong, H. De Bruyn, C. H. Such and B. S. Hawkett, *Australian Journal of Chemistry*, 2009, 62, 1501-1506.
134. Y. Yu, X. Zhan, Q. Zhang and F. Chen, *Polymer Engineering and Science*, 2011, 51, 1041-1050.
135. G. Holden, N. R. Legge, R. Quirk and H. E. Schroeder, *Thermoplastic elastomers*, 2nd edn., 1996.
136. P. Ganjeh-Anzabi, V. Haddadi-Asl, M. Salami-Kalajahi and M. Abdollahi, *Journal of Polymer Research*, 2013, 20, 248.
137. Z. Wang, Q. Zhang, X. Zhan, F. Chen, G. Rao and J. Xiong, *Journal of Polymer Research*, 2013, 20, 288.
138. J. Jennings, S. P. Bassett, D. Hermida-Merino, G. Portale, W. Bras, L. Knight, J. J. Titman, T. Higuchi, H. Jinnai and S. M. Howdle, *Polymer Chemistry*, 2016, 7, 905-916.
139. C. Farcet, B. Charleux and R. Pirri, *Macromolecules*, 2001, 34, 3823-3826.
140. J. Nicolas, B. Charleux, O. Guerret and S. P. Magnet, *Angewandte Chemie-International Edition*, 2004, 43, 6186-6189.
141. J. Nicolas, Y. Guillaneuf, C. Lefay, D. Bertin, D. Gigmes and B. Charleux, *Progress in Polymer Science*, 2013, 38, 63-235.
142. F. S. Bates and G. H. Fredrickson, *Annu. Rev. Phys. Chem.*, 1990, 41, 525-557.
143. L. Leibler, *Macromolecules*, 1980, 13, 1602-1617.
144. M. W. Matsen and F. S. Bates, *Macromolecules*, 1996, 29, 1091-1098.
145. N. A. Lynd, A. J. Meuler and M. A. Hillmyer, *Progress in Polymer Science*, 2008, 33, 875-893.
146. J. M. Widin, A. K. Schmitt, A. L. Schmitt, K. Im and M. K. Mahanthappa, *Journal of the American Chemical Society*, 2012, 134, 3834-3844.

147. M. W. Matsen, *Macromolecules*, 1995, 28, 5765-5773.
148. J. Bodycomb, D. Yamaguchi and T. Hashimoto, *Macromolecules*, 2000, 33, 5187-5197.
149. N. Singh, M. S. Tureau and T. H. Epps, *Soft Matter*, 2009, 5, 4757-4762.
150. I. Botiz and S. B. Darling, *Materials Today*, 2010, 13, 42-51.
151. T. Higuchi, A. Tajima, K. Motoyoshi, H. Yabu and M. Shimomura, *Angewandte Chemie-International Edition*, 2008, 47, 8044-8046.
152. M. M. Mok, J. Kim, C. L. H. Wong, S. R. Marrou, D. J. Woo, C. M. Dettmer, S. T. Nguyen, C. J. Ellison, K. R. Shull and J. M. Torkelson, *Macromolecules*, 2009, 42, 7863-7876.
153. D. Hermida-Merino, G. Portale, P. Fields, R. Wilson, S. P. Bassett, J. Jennings, M. Dellar, C. Gommès, S. M. Howdle, B. C. M. Vrolijk and W. Bras, *Review of Scientific Instruments*, 2014, 85.
154. M. Nomura and K. Suzuki, *Macromolecular Chemistry and Physics*, 1997, 198, 3025-3039.
155. P. B. Zetterlund, J. Wakamatsu and M. Okubo, *Macromolecules*, 2009, 42, 6944-6952.
156. Y. T. Li and S. P. Armes, *Angewandte Chemie-International Edition*, 2010, 49, 4042-4046.
157. S. Sugihara, A. Blanazs, S. P. Armes, A. J. Ryan and A. L. Lewis, *Journal of the American Chemical Society*, 2011, 133, 15707-15713.
158. G. Delaittre, M. Save, M. Gaborieau, P. Castignolles, J. Rieger and B. Charleux, *Polym Chem-Uk*, 2012, 3, 1526-1538.
159. J. M. Desimone, Z. Guan and C. S. Elsbernd, *Science*, 1992, 257, 945-947.
160. M. L. O'Neill, Q. Cao, R. Fang, K. P. Johnston, S. P. Wilkinson, C. D. Smith, J. L. Kerschner and S. H. Jureller, *Industrial & Engineering Chemistry Research*, 1998, 37, 3067-3079.
161. N. A. Birkin, N. J. Arrowsmith, E. J. Park, A. P. Richez and S. M. Howdle, *Polymer Chemistry*, 2011, 2, 1293-1299.
162. N. A. Birkin, O. J. Wildig and S. M. Howdle, *Polymer Chemistry*, 2013, 4, 3791-3799.
163. H. Lee, E. Terry, M. Zong, N. Arrowsmith, S. Perrier, K. J. Thurecht and S. M. Howdle, *Journal of the American Chemical Society*, 2008, 130, 12242-12243.
164. E. J. Beckman, *J. Supercrit. Fluids*, 2004, 28, 121-191.
165. M. Destarac, *Macromolecular Reaction Engineering*, 2010, 4, 165-179.
166. P. B. Zetterlund, G. Gody and S. Perrier, *Macromol. Theory Simul.*, 2014, 23, 331-339.
167. J. Vandenberg, T. d. m. Ogawa and T. Junkers, *Journal of Polymer Science Part a-Polymer Chemistry*, 2013, 51, 2366-2374.
168. C. J. Ferguson, R. J. Hughes, B. T. T. Pham, B. S. Hawkett, R. G. Gilbert, A. K. Serelis and C. H. Such, *Macromolecules*, 2002, 35, 9243-9245.
169. C. J. H. Ferguson, R. J.; Nguyen, D.; Pham, B. T. T.; Gilbert, R. G.; Serelis, A. K.; Such, C. H.; Hawkett, B. S., *Macromolecules*, 2005, 38, 2191-2204.
170. J. Rieger, F. Stoffelbach, C. Bui, D. Alaimo, C. Jerome and B. Charleux, *Macromolecules*, 2008, 41, 4065-4068.
171. C. Dire, S. Magnet, L. Couvreur and B. Charleux, *Macromolecules*, 2009, 42, 95-103.
172. S. Brusseau, J. Belleney, S. Magnet, L. Couvreur and B. Charleux, *Polym Chem-Uk*, 2010, 1, 720-729.
173. G. P. Zheng, C., *Macromolecules*, 2006, 39, 95-102.
174. W. M. Wan, C. Y. Hong and C. Y. Pan, *Chemical communications*, 2009, DOI: 10.1039/b912804b, 5883-5885.
175. W. M. Wan, X. L. Sun and C. Y. Pan, *Macromolecules*, 2009, 42, 4950-4952.
176. J. M. A. Blanazs, G. Battaglia, A. J. Ryan, S. P. Armes, *J. Am. Chem. Soc.*, 2011, 133, 16581-16587.
177. A. Blanazs, A. J. Ryan and S. P. Armes, *Macromolecules*, 2012, 45, 5099-5107.
178. N. J. Warren, O. O. Mykhaylyk, D. Mahmood, A. J. Ryan and S. P. Armes, *Journal of the American Chemical Society*, 2014, 136, 1023-1033.
179. J. N. Israelachvili, D. J. Mitchell and B. W. Ninham, *J Chem Soc Farad T 2*, 1976, 72, 1525-1568.
180. A. Blanazs, R. Verber, O. O. Mykhaylyk, A. J. Ryan, J. Z. Heath, C. W. Douglas and S. P. Armes, *Journal of the American Chemical Society*, 2012, 134, 9741-9748.
181. P. B. Zetterlund, S. C. Thickett, S. Perrier, E. Bourgeat-Lami and M. Lansalot, *Chemical reviews*, 2015, 115, 9745-9800.

182. N. J. Warren and S. P. Armes, *Journal of the American Chemical Society*, 2014, 136, 10174-10185.
183. B. Charleux, G. Delaittre, J. Rieger and F. D'Agosto, *Macromolecules*, 2012, 45, 6753-6765.
184. J. T. Sun, C. Y. Hong and C. Y. Pan, *Polym Chem-Uk*, 2013, 4, 873-881.
185. M. J. Derry, L. A. Fielding and S. P. Armes, *Progress in Polymer Science*, 2016, 52, 1-18.
186. S. L. Canning, G. N. Smith and S. P. Armes, *Macromolecules*, 2016, 49, 1985-2001.
187. D. Chan-Seng and M. K. Georges, *J Polym Sci Pol Chem*, 2006, 44, 4027-4038.
188. K. H. Kim, J. Kim and W. H. Jo, *Polymer*, 2005, 46, 2836-2840.
189. S. Sugihara, K. Sugihara, S. P. Armes, H. Ahmad and A. L. Lewis, *Macromolecules*, 2010, 43, 6321-6329.
190. S. Sugihara, S. P. Armes and A. L. Lewis, *Angewandte Chemie*, 2010, 49, 3500-3503.
191. W. X. Ji, J. J. Yan, E. Q. Chen, Z. C. Li and D. H. Liang, *Macromolecules*, 2008, 41, 4914-4919.
192. W. M. Cai, W. M. Wan, C. Y. Hong, C. Q. Huang and C. Y. Pan, *Soft Matter*, 2010, 6, 5554-5561.
193. W. D. He, X. L. Sun, W. M. Wan and C. Y. Pan, *Macromolecules*, 2011, 44, 3358-3365.
194. W. M. Wan and C. Y. Pan, *Macromolecules*, 2010, 43, 2672-2675.
195. W. M. Wan and C. Y. Pan, *Polym Chem-Uk*, 2010, 1, 1475-1484.
196. W. M. Wan, X. L. Sun and C. Y. Pan, *Macromolecular rapid communications*, 2010, 31, 399-404.
197. C. Q. Huang and C. Y. Pan, *Polymer*, 2010, 51, 5115-5121.
198. W. Zhao, G. Gody, S. M. Dong, P. B. Zetterlund and S. Perrier, *Polym Chem-Uk*, 2014, 5, 6990-7003.
199. S. M. Dong, W. Zhao, F. P. Lucien, S. Perrier and P. B. Zetterlund, *Polym Chem-Uk*, 2015, 6, 2249-2254.
200. H. Z. Chengqiang Gao, Yaqing Qu, Wei Wang, Habib Khan, and Wangqing Zhang, *Macromolecules*, 2016.
201. H. Zhou, C. G. Liu, C. Q. Gao, Y. Q. Qu, K. Y. Shi and W. Q. Zhang, *J Polym Sci Pol Chem*, 2016, 54, 1517-1525.
202. E. R. Jones, O. O. Mykhaylyk, M. Semsarilar, M. Boerakker, P. Wyman and S. P. Armes, *Macromolecules*, 2016, 49, 172-181.
203. W. Wang, C. Q. Gao, Y. Q. Qu, Z. F. Song and W. Q. Zhang, *Macromolecules*, 2016, 49, 2772-2781.
204. Y. Q. Qu, S. Wang, H. Khan, C. Q. Gao, H. Zhoua and W. Q. Zhang, *Polym Chem-Uk*, 2016, 7, 1953-1962.
205. Z. An, Q. Shi, W. Tang, C. K. Tsung, C. J. Hawker and G. D. Stucky, *Journal of the American Chemical Society*, 2007, 129, 14493-14499.
206. J. Rieger, C. Grazon, B. Charleux, D. Alaimo and C. Jerome, *J Polym Sci Pol Chem*, 2009, 47, 2373-2390.
207. W. Q. Shen, Y. L. Chang, G. Y. Liu, H. F. Wang, A. N. Cao and Z. S. An, *Macromolecules*, 2011, 44, 2524-2530.
208. P. B. Zetterlund, Y. Kagawa and M. Okubo, *Chemical reviews*, 2008, 108, 3747-3794.
209. S. W. Prescott, M. J. Ballard, E. Rizzardo and R. G. Gilbert, *Macromolecules*, 2002, 35, 5417-5425.
210. D. E. Ganeva, E. Sprong, H. de Bruyn, G. G. Warr, C. H. Such and B. S. Hawkett, *Macromolecules*, 2007, 40, 6181-6189.
211. J. Rieger, G. Osterwinter, C. O. Bui, F. Stoffelbach and B. Charleux, *Macromolecules*, 2009, 42, 5518-5525.
212. J. Ji, L. F. Yan and D. H. Xie, *J Polym Sci Pol Chem*, 2008, 46, 3098-3107.
213. I. Chaduc, W. Zhang, J. Rieger, M. Lansalot, F. D'Agosto and B. Charleux, *Macromolecular rapid communications*, 2011, 32, 1270-1276.
214. S. Boisse, J. Rieger, G. Pembouong, P. Beaunier and B. Charleux, *J Polym Sci Pol Chem*, 2011, 49, 3346-3354.
215. X. W. Zhang, S. Boisse, W. J. Zhang, P. Beaunier, F. D'Agosto, J. Rieger and B. Charleux, *Macromolecules*, 2011, 44, 4149-4158.



216. S. Boisse, J. Rieger, K. Belal, A. Di-Cicco, P. Beaunier, M.-H. Li and B. Charleux, *Chemical communications*, 2010, 46, 1950-1952.
217. W. Zhang, F. D'Agosto, O. Boyron, J. Rieger and B. Charleux, *Macromolecules*, 2012, 45, 4075-4084.
218. N. P. Truong, M. V. Dussert, M. R. Whittaker, J. F. Quinn and T. P. Davis, *Polym Chem-Uk*, 2015, 6, 3865-3874.
219. N. P. Truong, M. R. Whittaker, A. Anastasaki, D. M. Haddleton, J. F. Quinn and T. P. Davis, *Polym Chem-Uk*, 2016, 7, 430-440.
220. G. Delaittre, J. Nicolas, C. Lefay, M. Save and B. Charleux, *Chemical communications*, 2005, DOI: 10.1039/b415959d, 614-616.
221. G. Delaittre, J. Nicolas, C. Lefay, M. Save and B. Charleux, *Soft Matter*, 2006, 2, 223-231.
222. G. Delaittre and B. Charleux, *Macromolecules*, 2008, 41, 2361-2367.
223. P. B. Zetterlund, *Polym Chem-Uk*, 2011, 2, 534-549.
224. P. B. Zetterlund and M. Okubo, *Macromolecules*, 2006, 39, 8959-8967.
225. G. Delaittre, M. Save and B. Charleux, *Macromolecular rapid communications*, 2007, 28, 1528-1533.
226. R. McHale, F. Aldabbagh and P. B. Zetterlund, *J Polym Sci Pol Chem*, 2007, 45, 2194-2203.
227. J. N. Bernadette Charleux, and Olivier Guerret, *Macromolecules*, 2005, 38, 5485-5492.
228. G. Delaittre, C. Dire, J. Rieger, J. L. Putaux and B. Charleux, *Chemical communications*, 2009, DOI: 10.1039/b903040a, 2887-2889.
229. E. Groison, S. Brusseau, F. D'Agosto, S. Magnet, R. Inoubli, L. Couvreur and B. Charleux, *Acc Macro Lett*, 2012, 1, 47-51.
230. A. Darabi, P. G. Jessop and M. F. Cunningham, *Macromolecules*, 2015, 48, 1952-1958.
231. A. Darabi, A. R. Shirin-Abadi, J. Pinaud, P. G. Jessop and M. F. Cunningham, *Polym Chem-Uk*, 2014, 5, 6163-6170.
232. M. Okubo, Y. Sugihara, Y. Kitayama, Y. Kagawa and H. Minami, *Macromolecules*, 2009, 42, 1979-1984.
233. Y. Kitayama, A. Chaiyasat, H. Minami and M. Okubo, *Macromolecules*, 2010, 43, 7465-7471.
234. H. Moribe, Y. Kitayama, T. Suzuki and M. Okubo, *Macromolecules*, 2011, 44, 263-268.
235. Y. Kitayama, H. Moribe, H. Minami and M. Okubo, *Polymer*, 2011, 52, 2729-2734.
236. Y. Kitayama, H. Moribe, K. Kishida and M. Okubo, *Polym Chem-Uk*, 2012, 3, 1555-1559.
237. Y. Kitayama, K. Kishida and M. Okubo, *J Polym Sci Pol Chem*, 2013, 51, 716-723.
238. Y. Kitayama and M. Okubo, *Polym Chem-Uk*, 2014, 5, 2784-2792.
239. H. Moribe, Y. Kitayama, T. Suzuki and M. Okubo, *Polym J*, 2012, 44, 205-210.
240. J. J. Wu, H. J. Jiang, L. F. Zhang, Z. P. Cheng and X. L. Zhu, *Polym Chem-Uk*, 2016, 7, 2486-2491.
241. H. Yabu, *Bull. Chem. Soc. Jpn.*, 2012, 85, 265-274.
242. H. Yabu, T. Higuchi and H. Jinnai, *Soft Matter*, 2014, 10, 2919-2931.
243. Z. Jin and H. Fan, *Soft Matter*, 2014, 10, 9212-9219.
244. T. Higuchi, A. Tajima, H. Yabu and M. Shimomura, *Soft Matter*, 2008, 4, 1302-1305.
245. L. Li, K. Matsunaga, J. Zhu, T. Higuchi, H. Yabu, M. Shimomura, H. Jinnai, R. C. Hayward and T. P. Russell, *Macromolecules*, 2010, 43, 7807-7812.
246. S.-J. Jeon, G.-R. Yi, C. M. Koo and S.-M. Yang, *Macromolecules*, 2007, 40, 8430-8439.
247. S.-J. Jeon, G.-R. Yi and S.-M. Yang, *Advanced materials*, 2008, 20, 4103-4108.
248. K. H. Ku, H. Yang, J. M. Shin and B. J. Kim, *Journal of Polymer Science Part a-Polymer Chemistry*, 2015, 53, 188-192.
249. H. Yabu, T. Jinno, K. Koike, T. Higuchi and M. Shimomura, *Macromolecules*, 2011, 44, 5868-5873.
250. H. Yu, X. Qiu, S. P. Nunes and K.-V. Peinemann, *Nature Communications*, 2014, 5.
251. C.-S. Lim, J. H. Heo, M. S. You, S. H. Im and K. J. Chae, *Macromolecular Research*, 2014, 22, 324-328.
252. C. Allen, D. Maysinger and A. Eisenberg, *Colloids and Surfaces B-Biointerfaces*, 1999, 16, 3-27.
253. P. L. Soo and A. Eisenberg, *Journal of Polymer Science Part B-Polymer Physics*, 2004, 42, 923-938.

254. K. Kita-Tokarczyk, J. Grumelard, T. Haefele and W. Meier, *Polymer*, 2005, 46, 3540-3563.
255. P. Tanner, P. Baumann, R. Enea, O. Onaca, C. Palivan and W. Meier, *Accounts of chemical research*, 2011, 44, 1039-1049.
256. B. Karagoz, L. Esser, H. T. Duong, J. S. Basuki, C. Boyer and T. P. Davis, *Polymer Chemistry*, 2014, 5, 350-355.
257. M. Matsuguchi, N. Harada and S. Omori, *Sensor Actuat B-Chem*, 2014, 190, 446-450.
258. K. L. Thompson, C. J. Mable, J. A. Lane, M. J. Derry, L. A. Fielding and S. P. Armes, *Langmuir*, 2015, 31, 4137-4144.
259. A. Blanz, R. Verber, O. O. Mykhaylyk, A. J. Ryan, J. Z. Heath, C. W. I. Douglas and S. P. Armes, *Journal of the American Chemical Society*, 2012, 134, 9741-9748.
260. K. R. Phillips, G. T. England, S. Sunny, E. Shirman, T. Shirman, N. Vogel and J. Aizenberg, *Chemical Society reviews*, 2015, DOI: 10.1039/c5cs00533g.
261. P. Cotanda, N. Petzetakis and R. K. O'Reilly, *Mrs Communications*, 2012, 2, 119-126.
262. P. Tanner, P. Baumann, R. Enea, O. Onaca, C. Palivan and W. Meier, *Accounts of Chemical Research*, 2011, 44, 1039-1049.
263. S. P. Anthony, *Materials Letters*, 2009, 63, 773-776.
264. T. F. Jaramillo, S. H. Baeck, B. R. Cuenya and E. W. McFarland, *Journal of the American Chemical Society*, 2003, 125, 7148-7149.
265. M. J. Robb, L. A. Connal, B. F. Lee, N. A. Lynd and C. J. Hawker, *Polymer Chemistry*, 2012, 3, 1618-1628.
266. M.-K. Park, S. Jun, I. Kim, S.-M. Jin, J.-G. Kim, T. J. Shin and E. Lee, *Advanced Functional Materials*, 2015, 25, 4570-4579.
267. A. Nykanen, A. Rahikkala, S.-P. Hirvonen, V. Aseyev, H. Tenhu, R. Mezzenga, J. Raula, E. Kauppinen and J. Ruokolainen, *Macromolecules*, 2012, 45, 8401-8411.
268. A. Rahikkala, V. Aseyev, H. Tenhu, E. I. Kauppinen and J. Raula, *Biomacromolecules*, 2015, 16, 2750-2756.
269. S. J. Holder, G. Woodward, B. McKenzie and N. A. J. M. Sommerdijk, *Rsc Advances*, 2014, 4, 26354-26358.
270. D. Klinger, C. X. Wang, L. A. Connal, D. J. Audus, S. G. Jang, S. Kraemer, K. L. Killips, G. H. Fredrickson, E. J. Kramer and C. J. Hawker, *Angewandte Chemie-International Edition*, 2014, 53, 7018-7022.
271. L. Corte, V. Rebizant, G. Hochstetter, F. Tournilhac and L. Leibler, *Macromolecules*, 2006, 39, 9365-9374.
272. Z. J. Thompson, M. A. Hillmyer, J. Liu, H.-J. Sue, M. Dettloff and F. S. Bates, *Macromolecules*, 2009, 42, 2333-2335.
273. C. Cheng, N. Peduto, A. Hiltner, E. Baer, P. R. Soskey and S. G. Mylonakis, *Journal of Applied Polymer Science*, 1994, 53, 513-525.
274. K. H. Ku, J. M. Shin, M. P. Kim, C.-H. Lee, M.-K. Seo, G.-R. Yi, S. G. Jang and B. J. Kim, *Journal of the American Chemical Society*, 2014, 136, 9982-9989.
275. M. P. Kim, D. J. Kang, D.-W. Jung, A. G. Kannan, K.-H. Kim, K. H. Ku, S. G. Jang, W.-S. Chae, G.-R. Yi and B. J. Kim, *Acs Nano*, 2012, 6, 2750-2757.
276. K. H. Ku, M. P. Kim, K. Paek, J. M. Shin, S. Chung, S. G. Jang, W. S. Chae, G. R. Yi and B. J. Kim, *Small*, 2013, 9, 2667-2672.
277. E. Prodan, C. Radloff, N. J. Halas and P. Nordlander, *Science*, 2003, 302, 419-422.
278. M. Stefik, S. Guldin, S. Vignolini, U. Wiesner and U. Steiner, *Chemical Society reviews*, 2015, 44, 5076-5091.
279. L. A. Connal, N. A. Lynd, M. J. Robb, K. A. See, S. G. Jang, J. M. Spruell and C. J. Hawker, *Chem. Mat.*, 2012, 24, 4036-4042.
280. R. Jose, V. Thavasi and S. Ramakrishna, *Journal of the American Ceramic Society*, 2009, 92, 289-301.